2019

Petrology, Provenance, and Depositional Setting of the Lower Tallahatta Formation (Meridian Sand) in Grenada County, Mississippi

Husamaldeen Zubi
University of Mississippi

Recommended Citation

PETROLOGY, PROVENANCE, AND DEPOSITIONAL SETTING OF THE LOWER

TALLAHATTA FORMATION (MERIDIAN SAND) IN GRENADA COUNTY, MISSISSIPPI

A Thesis
presented in partial fulfillment of requirements
for the degree of Master of Science
in the Department of Geology and Geological Engineering
The University of Mississippi

By

Husamaldeen Zubi

December 2018

ABSTRACT

The Meridian Sand represents the lowermost member of the Middle Eocene Tallahatta Formation, which is found in the Gulf Coast region of the United States. Five stratigraphic sections in Grenada County were measured and described. Twenty-one sand and sandstone samples, and 2 mud samples were collected from all sections. Textural analyses were performed on all 23 samples to determine their lithologic properties. Petrographic descriptions and modal analyses were performed on thin sections made from the 21 sand and sandstone samples, and 400 grains were point counted in each sample. Geochemical analyses were carried out on all sand, sandstone, and mud samples using X-ray fluorescence (XRF) to identify elemental composition. X-ray diffraction (XRD) analyses were conducted to characterize the mineralogical composition of mud samples. Nine lithofacies were defined based on lithologic properties, and field observations. The general lithology of the Meridian Sand in Grenada County is very fine to coarse, angular to sub-angular, poorly to moderately well-sorted sand and sandstones, and it is often interbedded with mud beds. Quartz is the most dominant mineral, and it composes more than 90% of the framework grains in all sands and sandstones. The sands and sandstones were classified according to Dott's (1964) classification as quartzarenites, sublitharenites, quartzwackes, and lithicgraywackes.

Bulk geochemical analyses show that SiO_2 is the dominant compound with an average of 84.2% in all samples, whereas Zr is the dominant trace element, with an average value of ~318

 ppm. Ternary diagrams of modal analysis data following Dickenson (1985), indicate that the sands and sandstones of the Meridian Member were sourced from the craton interior or a recycled orogen province. Furthermore, plots of Th/Sc against Zr/Sc indicate a source from a sedimentary parent rock. Finally, sedimentary features such as mud drapes, lenticular bedding, flaser bedding, cross-bedding, and herringbone cross stratification, in addition to grain-size trends, indicate that the Meridian Sand was deposited in marginal-marine environments, including a tidal flat and shoreface settings.

LIST OF ABBREVIATIONS AND SYMPOLS

ME- Mississippi Embayment

Fm- Formation

PPM- Parts per million

ACKNOWLEDGMENT

First of all, I would like to thank my parents for the support they have provided during my journey through grade school. Without their support and kind words, I would not be able to do this job.

Second, I am deeply indebted to my advisor, Dr. Brian Platt. This thesis could not have been written without his essential advice, constructive comments and encouragement. He not only served me as a supervisor but also encouraged and challenged me throughout my academic program. Many thanks for him for his assistance with my fieldwork, lab work, and writing this thesis. I am furthermore highly grateful to Dr. Louis Zachos and Dr. Jennifer Gifford for accepting my request to serve as committee members and for their support, advice, and valuable hints. Also, I would like to thank Charles Swan for taking us around Grenada County to identify field sites.

In addition, I would like to thank the Libyan Ministry of Higher Education and Scientific Research for the financial support that helped me to achieve my master's degree in the US.

Finally, many thanks to the Geology and Geological Engineering Department for the support that helped me to complete this project.

LIST OF CONTENTS

LIST OF TABLES

LIST OF FIGURES

INTRODUCTION

The petrographic study of sands and sandstones can determine the properties and mineralogical composition of detrital grains, which can yield significant details about depositional environment, sediment transportation, provenance, and diagenetic history (Suttner, 1974). The mineralogical composition of sands and sandstones is influenced by the characteristics of the sediment source (Dickinson & Suczek, 1979) and can provide valuable information about whether these rocks are old or young, orogenic or anorogenic, or deposited far from or near to the source area (Garzanti, 2016). Provenance details of sedimentary rocks inferred from petrographic analyses can be complemented by bulk-sediment geochemistry (McLennan et al., 1993). Bulk-sediment geochemistry can also be useful for interpreting matrix-rich sandstones and fine-grained rocks and sediments, such as shales and silts. The small grain sizes of silts and clays, make it difficult to determine their provenance using petrographic techniques, but bulk geochemical analyses can determine their major and trace elements enabling interpretation of the composition of the source area (McLennan et al., 1993; Garzanti, 2016). Major element geochemistry has been used widely in provenance interpretations; however, the chemical composition of sandstones is a link not only to the parent rock, but also to diagenesis and chemical weathering (McLennan, 1989). Additionally, some trace elements, such as Zr and Sc, are not affected by chemical weathering or diagenesis and could reflect the properties of the parent rocks more faithfully (Bhatia & Crook, 1986; McLennan, 1989).

This project focuses on the Meridian Sand in Grenada County, Mississippi. The Meridian Sand is a productive aquifer in the Mississippi Embayment (Cushing et al., 1964), making its petrographic properties important for consideration of aquifer quality. Previous studies (e.g., Grim, 1936; Reynolds, 1992) of the Meridian Sand have focused more on depositional environment rather than provenance. Furthermore, the Meridian Sand has not yet been characterized petrographically.

This petrographic study was conducted to determine the mineralogical composition of the Meridian Sand, which can be used to understand the nature and composition of the source region. Petrography can also give important details about depositional processes when it is combined with textural analysis and stratigraphic relationships. The aim of this research is to use the petrology of the Meridian Sand Member of the middle Eocene Tallahatta Formation in Grenada County, Mississippi, to interpret the depositional environments and provenance of Meridian sediments.

GEOLOGIC SETTING

The Mississippi Embayment

The Mississippi Embayment (ME) of North America is a wide, southwestward-plunging syncline covering ~ 259,000 km^2 (Fig. 1), that spans portions of Texas, Louisiana, Alabama, Mississippi, Arkansas, Tennessee, Missouri, Illinois, and Kentucky (Cushing et al., 1964).

The early geologic history of the ME is poorly understood, and most of the information comes from geophysical data and deep well observations from the north portion of the ME. Such data from deep wells in northern Arkansas indicate that the Cambrian basal rocks of the ME are composed of unmetamorphosed red arkoses and granitic gneiss (Dension, 1984). ME basement rocks are overlain by Upper Cretaceous-Paleogene marine and marginal marine unconsolidated to poorly consolidated deposits. The thickness of these deposits reaches ~1 km in the north portion of the ME, where they overlie the Paleozoic facies of the Ozark platform. In the southern ME, the thickness of Upper Cretaceous-Paleogene deposits approaches ~2 km, where they overlie Paleozoic units of the Ouachita Mountains with an angular unconformity (Cook & Bally, 1975; Thomas, 1989). Near the Mississippi River, ~ 300 m of Cretaceous sedimentary rocks overlie Late Cambrian to Ordovician limestones, shales, and sandstones (Hildenbrand & Hendricks, 1995).

Stratigraphic, seismic, gravity, and petrologic observations show that the ME originated in the Late Proterozoic or early Paleozoic as a rift, known as the Reelfoot Rift, which was

reactivated during the Late Cretaceous. According to Ervin and McGinnis (1975), in the late Proterozoic, the area including the ME was uplifted due to emplacement of mantle plume into the basal crust. This uplift was one of the major tectonic events within North America in the late Precambrian (Burke & Dewey, 1973). The uplift was followed by erosion and tectonic activity that removed most of the deposits in the ME except arkosic sandstone and shale belts in western Missouri (Ham & Wilson, 1967). Subsidence of the uplifted area took place during the early Cambrian and continued through the Ordovician, resulting in sediment deposition over the former uplift. By the Ordovician, the mantle plume below the rift moved laterally and initiated the Nashville and Ozark domes (Ervin & McGinnis, 1975). These two domes were connected by the Ozark arch at the end of the early Paleozoic. Paleozoic rocks of the ME underwent erosion during the early and middle Mesozoic, followed by deposition of sediments in the Great Plains and Gulf of Mexico (Ervin & McGinnis, 1975). The construction of the present embayment began in the early Late Cretaceous as a result of the reactivation of Reelfoot Rift. This reactivation was accompanied by igneous syenite intrusions located along the ME axis (Ervin & McGinnis, 1975). An alternate interpretation is provided by Cox and Van Arsdale (1997), who suggest that the ME started to develop during the mid-Cretaceous as a thermally driven rift. They suggest that the ME uplifted as a result of the region passing over the Bermuda hotspot (Cox & Van Arsdale, 2002). This uplift was followed by erosion and subsidence of the ME (Cox and & Arsdale, 1997; 2002). Subsidence of the ME continued during the Cenozoic, although there is no evidence of igneous activity after the Cretaceous (Stearns and Marcher, 1962). Geophysical data show that the subsidence of the ME continues to the present time (McGinnis, 1963). Stearns and Wilson (1972); however, argued that the ME became stable after the last Neogene uplift.
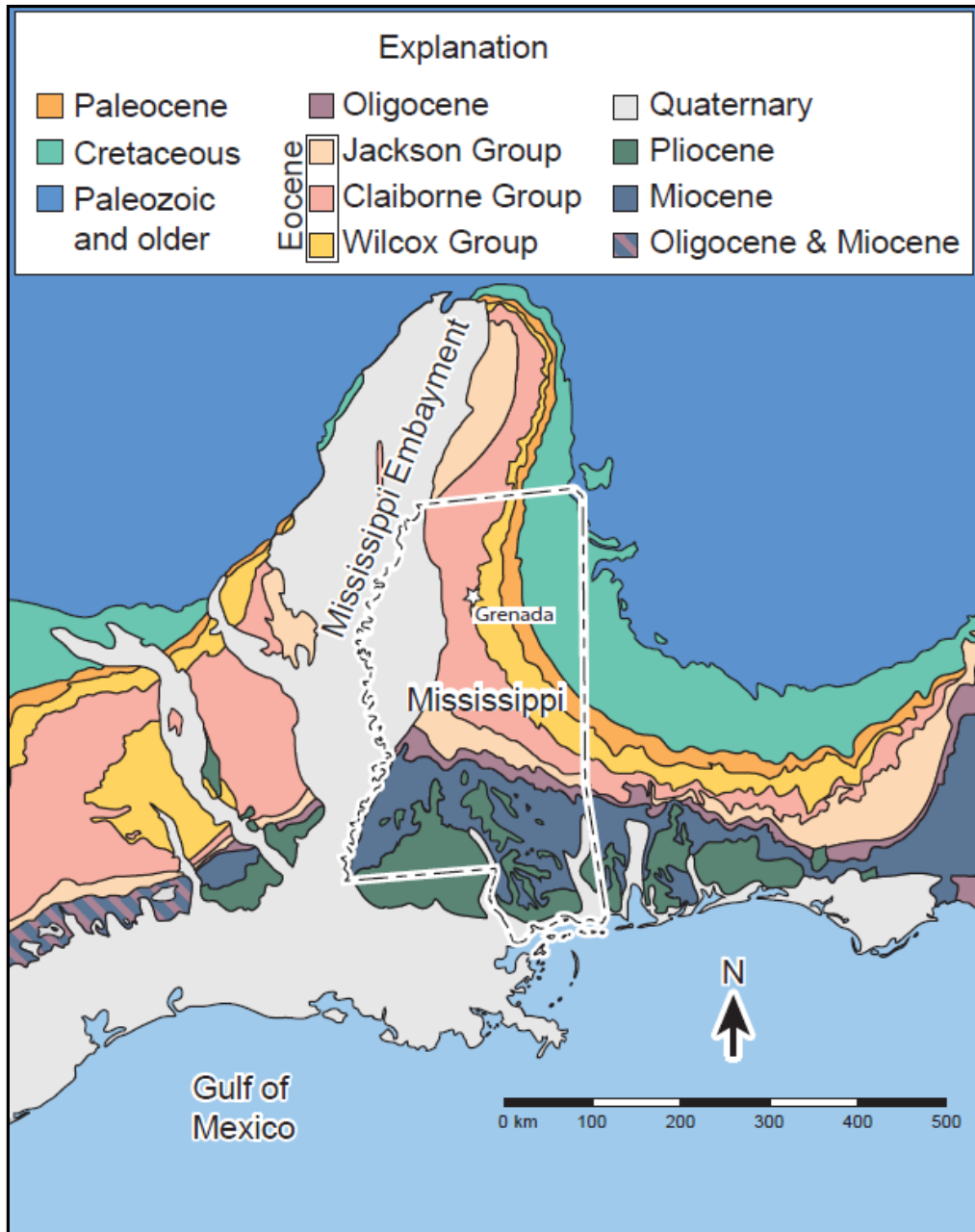
Figure 1. A map showing the Mississippi Embayment including Grenada County; modified from Reed et al. (2004).

Eocene stratigraphy of northern Mississippi

Eocene deposits of the Mississippi Embayment (ME) are divided into three lithostratigraphic groups. These groups are, in stratigraphic order, the Wilcox Group, the Claiborne Group, and the Jackson Group (Cushing et al., 1964). The Wilcox and Claiborne Groups are exposed at the surface in the north-central and northeastern portions of Mississippi, whereas the Jackson Group is exposed only in the south-central part of the state (Fig. 2) (Dockery & Thompson, 2016; Cushing et al., 1964).

The upper Paleocene-lower Eocene Wilcox Group contains thick successions of clastic deposits, and a significant proportion of these terrestrial deposits fill the western Gulf Coast province (Fisher & McGowen, 1967). In the subsurface of northern Mississippi, the Wilcox Group is dominated by two distinct lithologic units: a lower sand unit and an upper shale unit (Cushing et al., 1964). The Wilcox Group in the northern portion of Mississippi consists of, in ascending order, the Nanafalia Formation (Fm), the Tuscahoma Fm, the Bashi Fm, and the Hatchetigbee Fm. The Wilcox Group is underlain by marine carbonate and clastic sediments of the Midway Group and is overlain by limestone and clastic deposits of the Claiborne Group (Cushing et al.,1964; Dockery & Thomson, 2016).

The Eocene Claiborne Group consists mainly of marine and nonmarine sand, sandy clay, shale, and limestone. The thickest deposits of the Claiborne Group occur in the subsurface in the south portion of the ME, where they are ~ 792 m thick (Cushing et al., 1964). The sedimentary rocks of the Claiborne Group in Mississippi exhibit depositional cycles that alternate between deltaic and marine sedimentation. In Mississippi, five formations compose the Claiborne Group:

the Tallahatta Fm, the Winona Fm, the Zilpha Fm, the Cook Mountain Fm, and the Cockfield Fm (Dockery & Thompson, 2016).
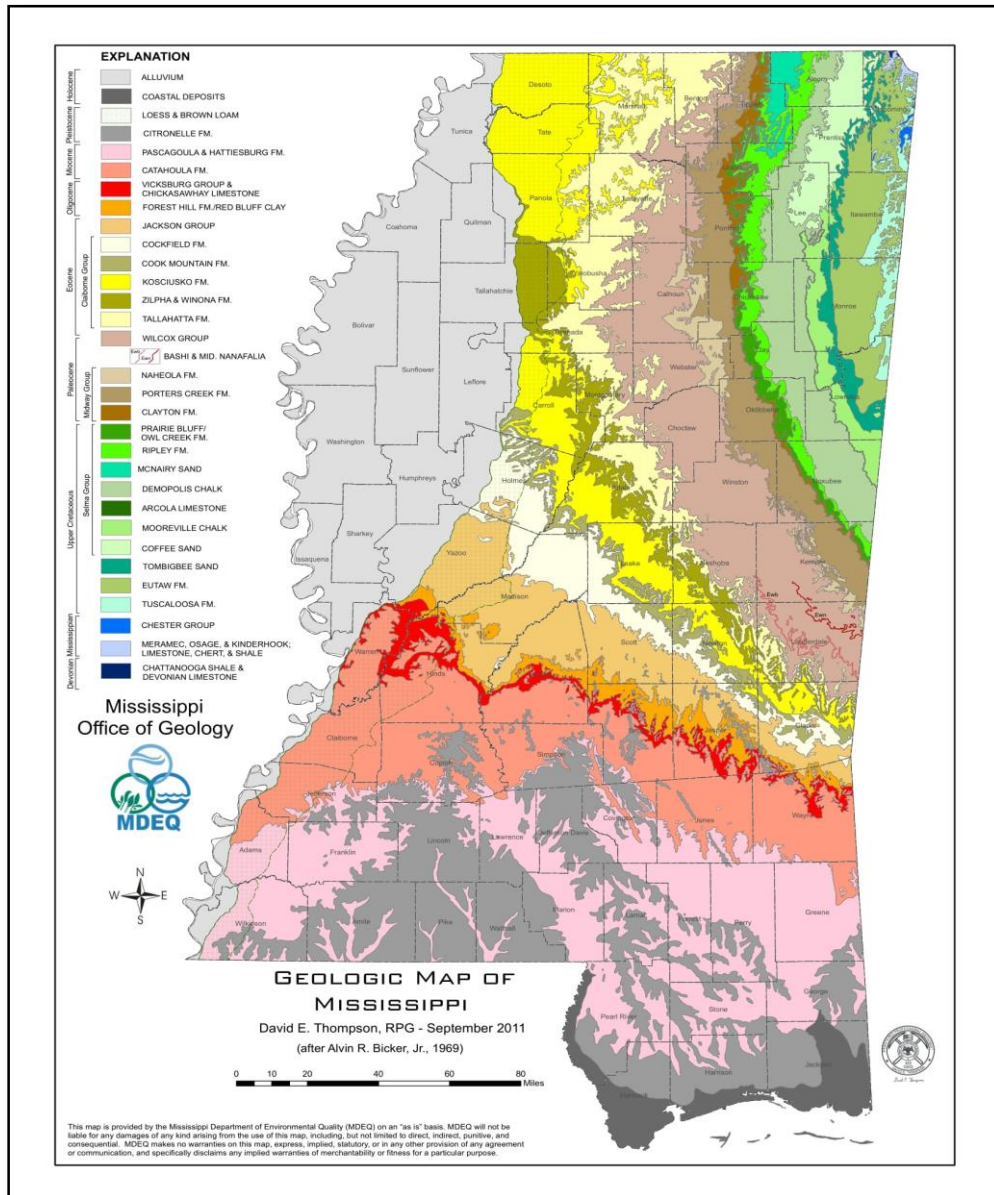
Figure 2. Geological map of Mississippi showing the Tallahatta Formation (light yellow) in north-central Mississippi (Dockery & Thompson, 2016).

Tallahatta Formation

The middle Eocene Tallahatta Fm is the basal unit of the Claiborne Group (Fig. 3), and it is exposed at the surface in a band that extends from western Georgia eastward across southern Alabama and through Mississippi. The Tallahatta Fm in Mississippi is underlain unconformably by the lower Eocene Hatchetigbee Fm of the Wilcox Group and overlain unconformably by the middle Eocene Winona Fm (Savrda et al., 2010). In Alabama, the Tallahatta Fm is overlain by the Lisbon Formation and underlain by the Hatchtigbee Fmof the Willcox Group (Fig. 3) (Bybell & Gibson, 1985). The age of the Tallahatta Fm is estimated to be early middle Eocene based mainly on mollusc assemblages (Toulmin, 1977). The Tallahatta Fm in western Georgia and eastern Alabama is thinner in comparison to west Alabama and Mississippi, and it is not divided into members (Savrda et al., 2010). In the western portion of Alabama, the formation is divided into the Meridian and Basic City Members, whereas it comprises the Meridian, Basic City, and Neshoba Members in central Mississippi (Fig. 3) (Cushing et al., 1964).

The Meridian Sand was named by Low (1933) for an exposure at Sey-mour's Hill south of Meridian, MS. The Meridian Sand crops out in western Alabama and Mississippi, and it is equivalent to the Carrizo Sand of Arkansas, Louisiana, and Texas (Lowe, 1933). In initial studies, the Meridian Sand has been considered to be both a formation and a member. Thomas (1942) considered the Meridian Sand to be part of the Wilcox Group and he excluded it from the Tallahatta Fm because it is lithologically more similar to the underlying Wilcox Group than the overlying Claiborne Group. Murray (1961) also excluded the Meridian Sand from the Tallahatta Fm and placed it in the Wilcox Group based on its lithologic similarities.

The maximum thickness of the Meridian Sand is 149 m in the subsurface in Holmes County, Mississippi (Brown, 1947). In Grenada County, the thickness of the Meridian Sand varies from 23 m in the southern portion of the county to ~30 m at Grenada Lake (Adams, 1943). Generally, the lithology of the Meridian Sand is fine to very coarse cross-bedded to massive quartz sand (Cushing et al., 1964). The contact between the Meridian Sand Member (Claiborne Group) and the Hatchitigbee Formation (Wilcox Group) is usually sharp and determined by the presence of clay or shale in the Wilcox (Cushing et al., 1964). The depositional environment of the Meridian Sand was interpreted by Grim (1936) as a nearshore marine setting with wave action sufficient to perform considerable sorting. Reynolds (1991) interpreted the Meridian Sand as representing deposition in shoreface and foreshore beach environments.

The Basic City Member, which represents the middle member of the Tallahatta Fm in Mississippi and the upper member of the Tallahatta Fm in Alabama (Fig. 3), consists of fossiliferous light-colored claystone, siltstone, and shale (Cushing et al.,1964). The member was named by Lowe (1915) for an exposure just north of Basic City in Clark County, Mississippi.

The Meridian Sand Member overlies the Basic City Member, and their contact represents a regional disconformity that extends from western Alabama to western Mississippi (Thomas, 1942). The thickness of the Basic City Member averages ~30-38 m, in eastern Mississippi and it decreases towards central Mississippi, where it has an average thickness of 15-18 m (Thomas, 1942). The depositional environment of the Basic City Member has been interpreted as a relatively shallow marine setting (Grim, 1936). Merrill et al. (1985) interpreted the Basic City to be deposited in marine shelf and strandplain environments.

The Neshoba Sand was named by Thomas (1942), who described an exposure in southern Neshoba County, MS above the Basic City Member and below the Winona Sand Fm. It is the

9

uppermost member of the Tallahatta Fm in Mississippi and is composed typically of fine-grained, and well-sorted micaceous quartz sand. The Neshoba Sand Member has a thickness of about 15 m in central Mississippi, and it increases in thickness gradually towards northern Mississippi, where it approaches 42 m (Thomas, 1942). Stentzel (1952) suggested that the Neshoba Sand Member was equivalent to the Queen City Sand Member of the Mount Selman Fm in Texas. The Neshoba Sand was interpreted to be deposited in deltaic and strandplain environments (Merrill et al., 1985).

System	Series		Lithologic Units		
				Mississippi	Alabama
Paleogene	Eocene	Middle — Claiborne Group	Cockfield Formation		Gosport Formation
			Cook Formation		
			Sparta Formation		Lispon Formation
			Zilpha Formation		
			Winona Formation		
			Tallahatta Formation	Neshoba Sand	Tallahatta Formation / Basic City
				Basic City	
				Meridian Sand	Meridian Sand
	Lower — Willcox Group		Hatchetigbee Formation		Hatchetigbee Formation
			Bashi Formation		Bashi Formation

Figure 3. Generalized lower to middle Eocene stratigraphy of Mississippi and Alabama (Modified from Murray, 1961).

Location of study area

     Five locations in Grenada County, MS (Fig. 4) were selected for this project due to the availability of a number of relatively thick exposures that can provide vertically continuous outcrop data. In addition, the areal extent of these sections allow for the evaluation of lateral variations within the unit. The locations of the studied stratigraphic sections are illustrated in Figure 4B. Section 1 is located on the southwestern edge of Grenada Lake on State Highway 333. Section 2 is located to the west of Camp McCain, 320 m east of Interstate 55. Section 3 is located 800 m north of the Nat G.Troutt Rd, west of Camp McCain. Sites 4 and 5 are located along Highway 8, east of Interstate 55.
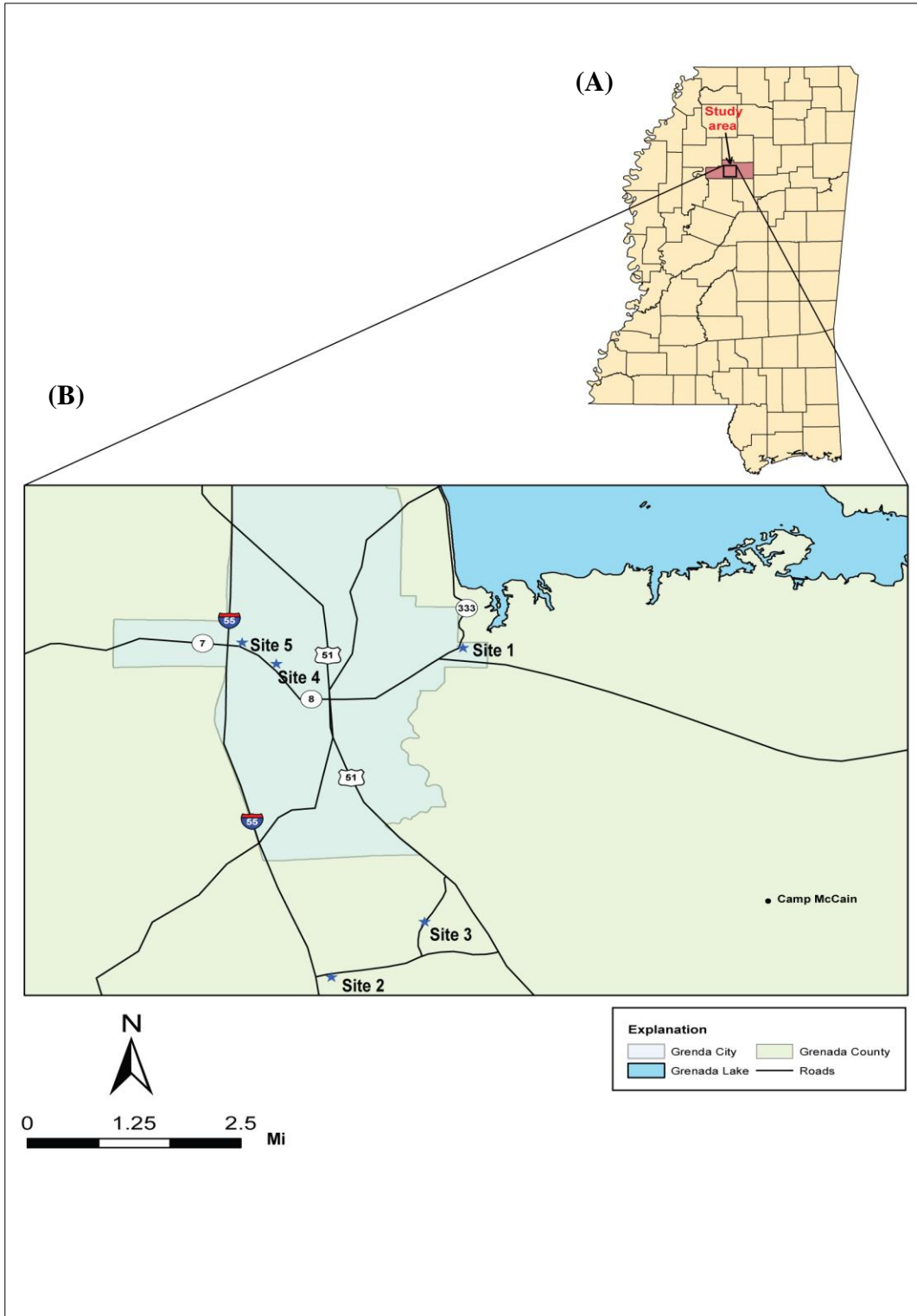
Figure 4. (A), a map showing the location of the study area. (B), a map of shaded area in A showing the five sites studied.

METHODS AND MATERIALS

Field Work

One stratigraphic section was measured at each of the field sites. Each section was measured using a tape measure and divided into beds or lithofacies as appropriate. Sedimentary structures, thicknesses, and contact types were described and recorded. Twenty-three bulk sand, sandstone, and mud samples were collected from the 5 sections based on the vertical variations in each section: six samples from section 1, six samples from section 2, three samples from section 3, two samples from section 4, and six samples from section 5. The locations and stratigraphic positions of all samples can be seen in Table 1.

Lab Work

Thin-sections with blue epoxy impregnation were made for all sand and sandstone samples. Each thin-section was described in detail, and modal analysis was performed by point counting 400 grains from each sample following Dickenson & Suczek (1979). Grain shape, and diagenetic features were described from thin-sections and documented. Particle-size distributions for friable sand and mud samples collected from the five sections were determined using a sieve shaker and standard sieve set. Sieves with openings of 1.0, 0.500, 0.250, 0.125, and 0.63 mm were used to correspond to the major breaks between sand classes and mud according to the

Udden–Wentworth scale. The grain size of the sandstone samples was determined using a stage micrometer because they are well cemented and can not be disaggregated for sieving.

Mean grain size, standard deviation (sorting), skewness, and kurtosis of particle size distributions of sand and mud samples were determined using the following equations (Blott and Pye, 2001):

(1) Mean
$$\bar{x}\emptyset = \frac{\sum fm\emptyset}{100}$$

(2) Standard deviation
$$\sigma\emptyset = \sqrt{\frac{\sum f(m\emptyset - \bar{x}\emptyset)^2}{100}}$$

(3) Skewness
$$sk\emptyset = \frac{\sum f(m\emptyset - \bar{x}\,\emptyset)^3}{100\sigma\emptyset^3}$$

(4) Kurtosis
$$k\emptyset = \frac{\sum f(m\emptyset - \bar{x}\,\emptyset)^4}{100\sigma\emptyset^4}$$

Where f is the weight or the number of each grain size in percent and m is midpoint of each grain size grade in phi values.

X-ray fluorescence (XRF) was performed on each sample to determine elemental abundances, which can be useful for distinguishing certain aspects of provenance (McLennan et al., 1993). Analyses were performed on a Thermo Quanx- EC device. Each sample was scanned three times for 500 seconds per scan, and then the mean was determined and recorded. Major oxide values obtained from XRF were normalized to 100% and recorded.

The mineralogical composition of the two mud samples was determined using X-ray diffraction (XRD). For each sample, 40 g were dried for 24 hours and then crushed into small pieces using a jaw crusher machine, and then powdered using a powder mill. Each sample was placed on a quartz plate and inserted into the D2 PHASER device without any additional treatment. After generating an x-ray beam, the detector moved around the sample in a circle recording x-rays in different angles. This step took ~40 minutes for each sample. XRD spectra recorded by the detector were then exported to MDI's Jade 2010 software to identify the individual minerals in each sample.

Table 1. The locations of the five sites, and the stratigraphic positions of the twenty-three samples.

Site Number	Sample ID	Stratigraphic Position (m)	Longitude	Latitude
1	M1-01	0.80	-89.767840°	33.785475°
1	M1-02	4.25	-89.767840°	33.785475°
1	M1-03	4.60	-89.767840°	33.785475°
1	M1-04	5.10	-89.767840°	33.785475°
1	M1-05	6.15	-89.767840°	33.785475°
1	M1-06	7.10	-89.767840°	33.785475°
2	M2-01	0.70	-89.809008°	33.683639°
2	M2-02	1.55	-89.809008°	33.683639°
2	M2-03	2.20	-89.809008°	33.683639°
2	M2-04	2.85	-89.809008°	33.683639°
2	M2-05	3.35	-89.809008°	33.683639°
2	M2-06	3.90	-89.809008°	33.683639°
3	M3-01	0.20	-89.781964°	33.696616°
3	M3-02	1.25	-89.781964°	33.696616°
3	M3-03	1.95	-89.781964°	33.696616°
4	M4-01	0.75	-89.824984°	33.780263°
4	M4-02	2.35	-89.824984°	33.780263°
5	M5-01	0.40	-89.835731°	33.786631°
5	M5-02	0.70	-89.835731°	33.786631°
5	M5-03	0.95	-89.835731°	33.786631°
5	M5-04	1.55	-89.835731°	33.786631°
5	M5-05	2.15	-89.835731°	33.786631°
5	M5-06	2.85	-89.835731°	33.786631°

RESULTS

Measured Sections

Section 1

Section 1 (Fig. 5) was measured at an exposure on the southern edge of Grenada Lake on MS State Highway 333 (Fig. 4) at latitude 33.785475°N and longitude -89.767840°W. This section has a thickness of 7.86 m, and it contains 5 lithofacies (Fig. 6). Beds in this section are dominantly sands, particularly at the bottom and the top of the exposure. Muds are present within the middle of the exposure. The sand is very fine to fine, moderately to moderately well sorted, angular to sub-angular.

Section 2

Section 2 (Fig. 7) is exposed east of Interstate 55, to the west of Camp McCain (Fig. 4) at latitude 33.683639°N and longitude -89.809008° W. The thickness of this section is 4.55 m, and it is divided into 4 lithofacies (Fig. 8). This exposure is composed mainly of sand and sandstone with a minor amount of thin mud deposits at the lower middle part of the exposure. Mud lenses and clasts are present within the sand deposits, particularly at the bottom and the top of the exposure. The sand and sandstone consist mostly of fine to medium, moderately to moderately well sorted, angular to sub-angular grains.

Figure 5. Section 1 within the Meridian Sand, southwest Grenada Lake, Grenada County, MS.
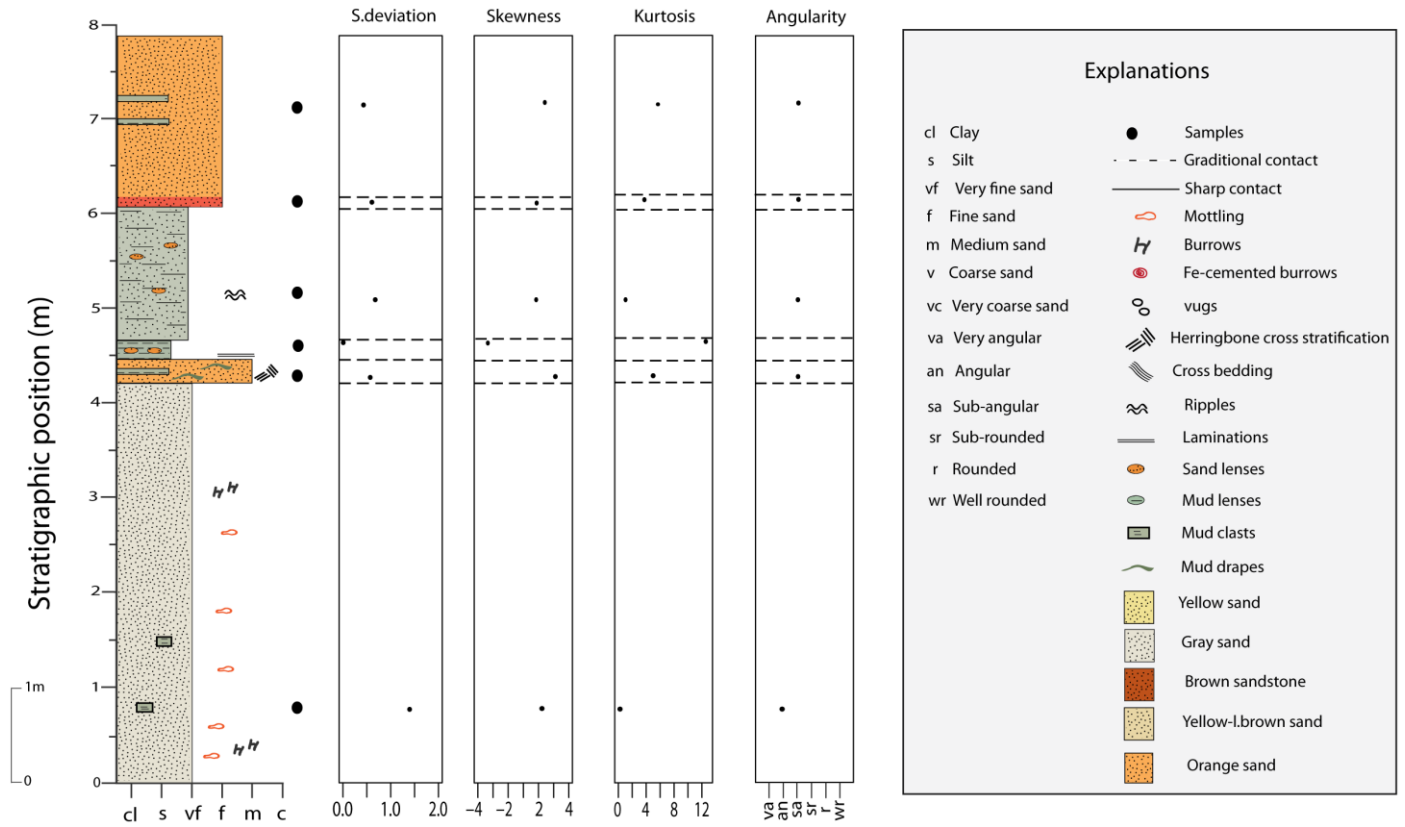
Figure 6. Stratigraphic column of Section 1, southwest of Grenada Lake, Grenada County, MS. Mud clast and sand lens sizes are not to scale.

20

Figure 7. Section 2 within the Meridian Sand, west Camp McCain, east of Interstate 55, Grenada County, MS.
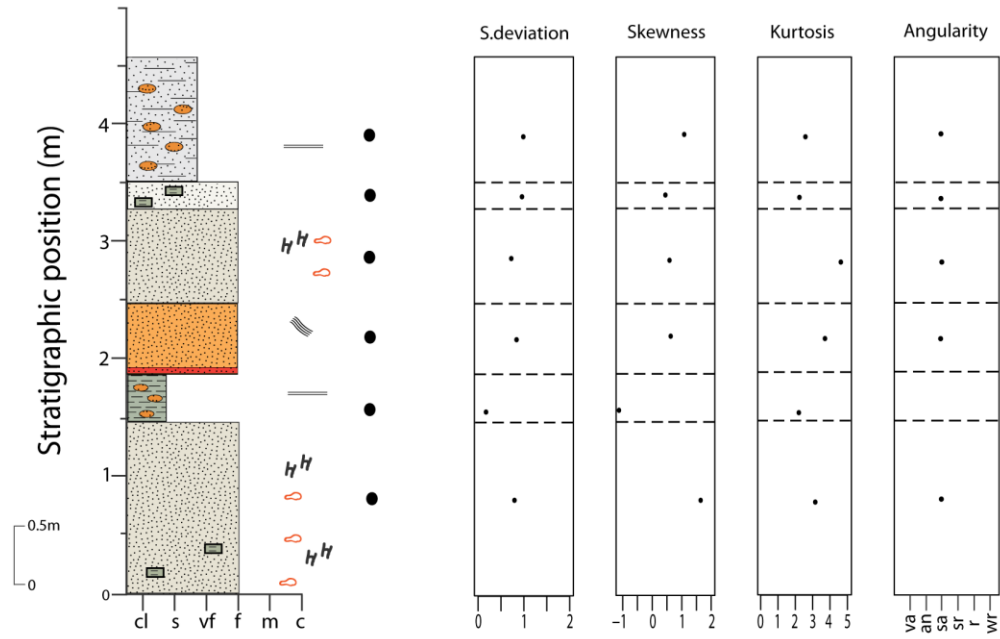
Figure 8. Stratigraphic column of section 2, west Camp McCain, east of Interstate 55, Grenada County, MS. Mud clast and sand lens sizes are not to scale. See Figure 6 for explanation of symbols.

Section 3

This section (Fig. 9) is exposed to the north of Nat G Troutt Road, west of Camp McCain (Fig. 4) at 33.696616°N and -89.781964° W. The thickness of this section is 2.68 m, and it contains 2 lithofacies (Fig. 10). This exposure is composed mostly of very fine, moderately sorted, sub-angular sand with some mud clasts at the base of the exposure. At the upper part of the exposure, the sand is medium sized, moderately well sorted and sub-angular, and it contains mud lenses.

Figure 9. Section 3 within the Meridian Sand, west of Camp McCain, north of the Nat G Troutt Rd, Grenada County, MS.

Section 4

Section 4 (Fig. 11) is exposed along Highway 8, east of Interstate 55 (Fig. 4) at

33.780263°N and 89.824984°W (Fig. 4). The thickness of this section is ~3.1 m, and it contains

2 lithofacies (Fig. 12). The exposure is composed of sandy sediments with some mud clasts in

the lower part of the exposure. The sand is composed of light gray to yellow, very fine to fine,

moderately well sorted, and mostly sub-angular grains.

Section 5

Section 5 (Fig. 13) is exposed along Highway 8, east of Interstate 55 (Fig. 4), just behind

the Quality Inn hotel at 33.786631°N and 89.835731°W. The thickness of this exposure is 3.15

m, and it is divided into 3 lithofacies (Fig. 14). The lithology of this exposure is light gray to

yellow sand that alternates with highly bioturbated dark red to brown sandstone. This exposure

shows a coarsening upward trend from fine sand at the bottom of the exposure to red coarse

sandstone in the middle of the exposure. In the upper part of this section, the lithology changes

from fine sand to coarse sandstone. The sand and sandstone contain poorly to moderately sorted,

angular to sub-angular grains.
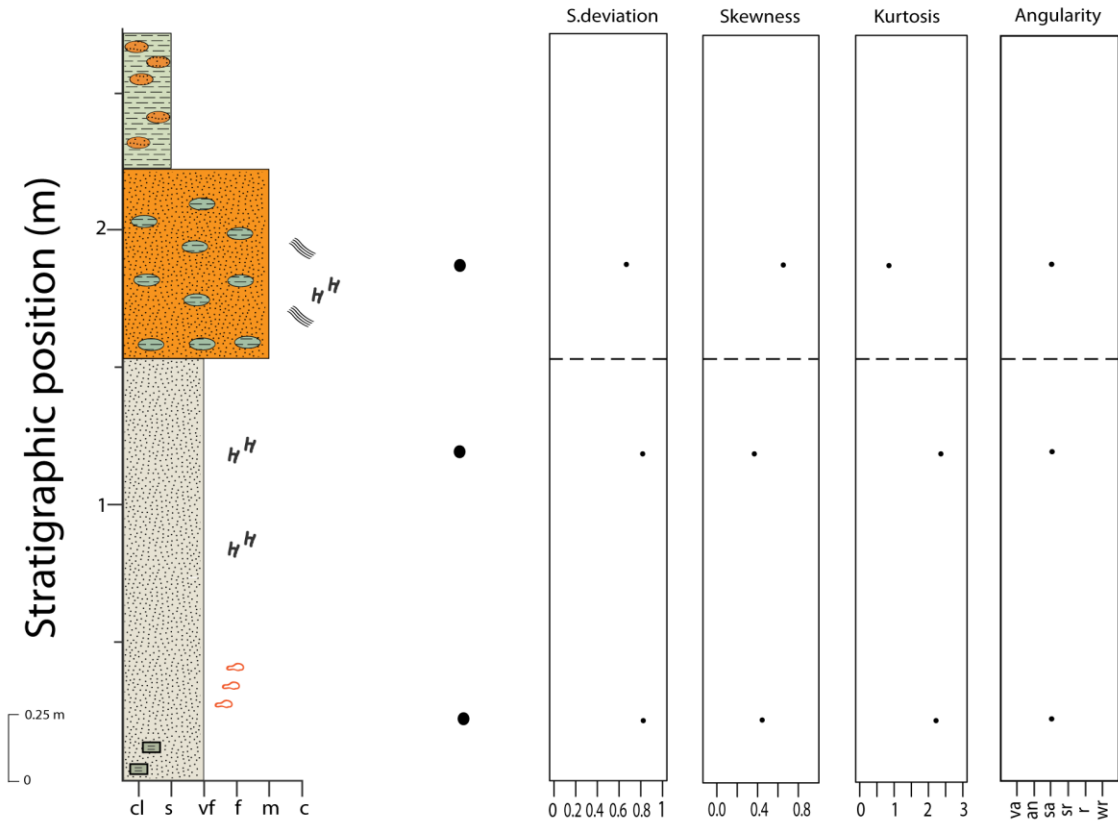
Figure 10. Stratigraphic column of section 3, west of Camp McCain, north of the Nat G. Troutt Rd, Grenada County, MS. Mud clast and mud lens sizes are not to scale. See Figure 6 for explanation of symbols.

Figure 11. Section 4 within the Meridian Sand, along Highway 8, east of Interstate 55, Grenada County, MS.
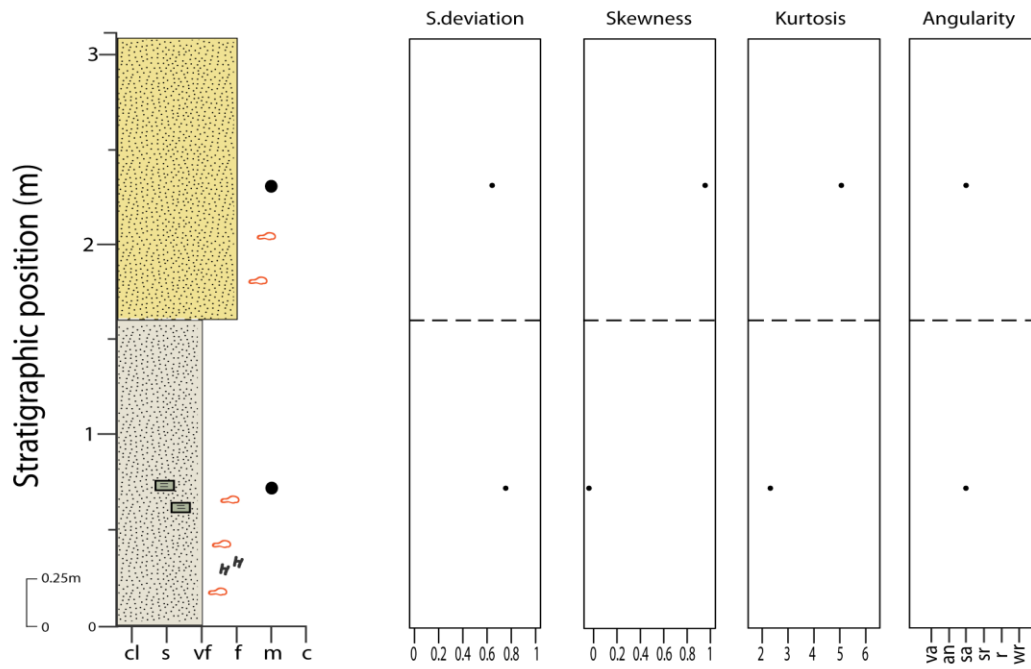
Figure 12. Stratigraphic column of section 4 within the Meridian Sand, along Highway 8, east of Interstate 55, Grenada County, MS. Mud clasts not to scale. See Figure 6 for explanation of symbols.

Figure 13. Section 5 within the Meridian Sand, along Highway 8, east of Interstate 55, Grenada County, MS.
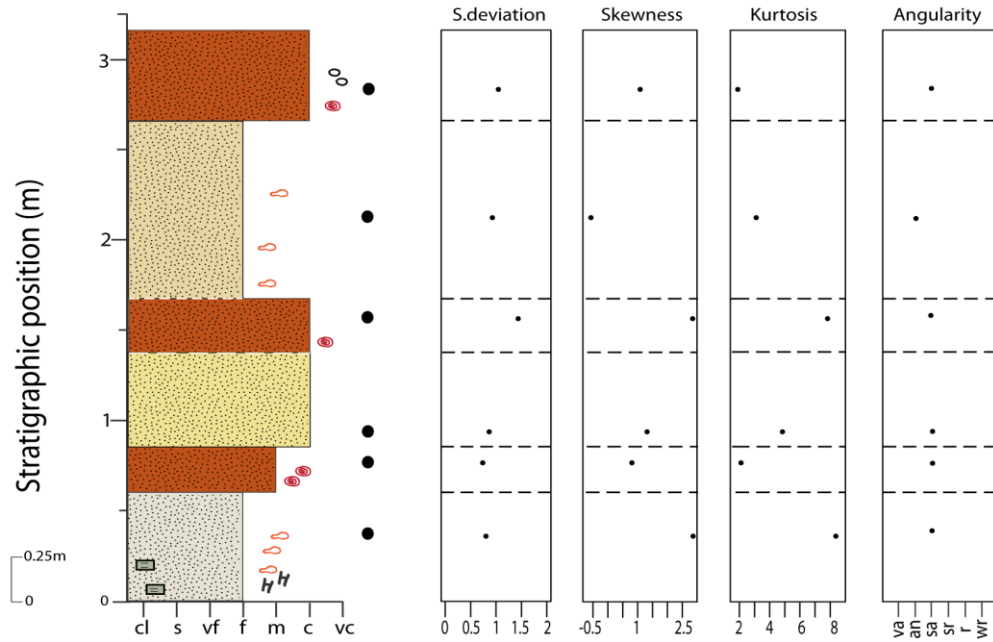
Figure 14. Stratigraphic column of section 5 within the Meridian Sand, along Highway 8, east of Interstate 55, Grenada County, MS. Mud clasts are not to scale. See Figure 6 for explanation of symbols.

Lithofacies Descriptions

Nine lithofacies are recognized within the Meridian Sand in Grenada County based on mean grain-size, sorting, and sedimentary features. Grain size data for all lithofacies are provided in Table 2.

Lithofacies 1

This lithofacies consists of sand and beds that range in thickness from 1.56 to 3.95 m. The sand is very fine with an average grain size of 3.16 ɸ and maximum grain size of > 1 ɸ. The standard deviation of the particle size distribution of this lithofacies ranges from 0.76 to 0.83 ɸ (Moderately sorted) (Folk, 1980). Skewness values range from -0.04 to 0.40 ɸ (fine skewed to symmetrical) and kurtosis values range from 2.38 to 2.45 ɸ (platykurtic). Sand from this lithofacies is mostly sub-angular with 10% angular grains and 20% are sub-rounded grains. Also, the majority of the grains are highly spherical. The sand is texturally submature to mature.

The sand from this lithofacies is light gray to light yellow. It lacks sedimentary structures, and it is mostly massive. There are some mud clasts within the lithofacies that range in diameter from 1-4 cm. These clasts are distributed mostly at the base of the lithofacies (Fig. 15). This lithofacies also contains color mottling. This lithofacies is overlain by lithofacies 13 in section 3 and lithofacies 3 in section 4 by sharp and gradational contacts, respectively.

Figure 15. Gray mud clast (red arrow) within lithofacies 1; 28-cm-long spade for scale.

Lithofacies 2

This lithofacies is the thickest bedded (up to 4.2 m) of all the lithofacies. It consists of light gray, very fine sand with a mean grain size of 3.03 ɸ and a maximum grain size of >2 ɸ. The sand is poorly sorted with a standard deviation value of 1.31 ɸ. Skewness and kurtosis values are 0.08 ɸ and 0.148 ɸ, which are symmetrical and very platykurtic, respectively. Sand

from this lithofacies is characterized by a muddy matrix, which makes up ~ 7% of the total

sample observed.

Bedding is massive with some burrows that are distributed at the lower and upper part of

beds (Fig. 16). Furthermore, this lithofacies contains mud clasts that are 1-2 cm thick. There is

also color mottling that can be seen throughout the entire lithofacies.

Figure 16. Burrows (red arrows) and mottling (blue arrows) in lithofacies
2; 28-cm-long spade for scale.

The sand grains from this lithofacies are mostly sub-angular (~70%), while the other 30 % are sub-rounded and angular. Seventy percent of the grains have low sphericity, and the remainder is highly spherical. The sand is texturally submature.

Lithofacies 3

This lithofacies is present in sections 1 and 2, where it has an average thickness of 1.3 m. It consists of light gray muddy sand with a mean grain-size of 3.43 φ and a maximum grain size of >2.5 φ. The standard deviation values in this lithofacies range from 0.75 to 0.99, which indicates moderate sorting (Folk, 1980). The skewness ranges from -0.09 to 1.51 φ (symmetrical to fine skewed) and kurtosis values range from 0.45 and 2 φ (very platykurtic). The mud-sized materials in this lithofacies make up ~29% of the total sediments. Most of the grains (~80 %) are sub-angular, and 20% are angular. Forty percent of the sand grains have low sphericity and 60% have high sphericity. This lithofacies is characterized texturally by immature sand.

This lithofacies is characterized by wave ripples, particularly near the base, and it also contains some orange sand lenses that are up to 1 cm thick (Fig. 17). The lithofacies is overlain by lithofacies 4 with a sharp contact.

Lithofacies 4

This lithofacies is present in sections 1 and 4, and it consists of light yellow to dark orange sand. The average thickness of this lithofacies is ~1.6 m. The sand is very fine, and it has a mean grain size of 2.65 φ, and a maximum grain size of >1 φ. The sand is moderately well sorted, and the standard deviation values range from 0.59 to 0.71 φ. The skewness values range from -0.23 to 0.43 φ (fine to coarse skewed) and kurtosis ranges from 4.29 to 5.68 φ

(leptokurtic). The sand grains from this lithofacies are mainly sub-angular with 25% angular and 10% sub-rounded. Seventy percent of the grains have high sphericity, while the remainder has low sphericity. The sand from this lithofacies is texturally submature to mature.

The lithofacies is mostly massive with very thin mud beds. There is some color mottling, particularly at the bottom of beds in this lithofacies. The lithofacies is exposed at the upper part of sections 1 and 4, and it is underlain by lithofacies 3 with a sharp contact and lithofacies 1 by a gradational contact.

Lithofacies 5

This lithofacies is present in sections 2 and 5. In section 2, the thickness of this lithofacies is ~ 1.7 m. In section 5, this lithofacies is found in three different stratigraphic positions, and its thickness ranges from 0.5 to 0.8 m. The sand is white, light gray to orange. The mean grain size of this sand is 2.54 ϕ, while the maximum grain size is >1 ϕ. The standard deviation of the grains in this lithofacies ranges from 0.73 to 0.92 ϕ, which classifies the sand as moderately sorted (Folk, 1980). The sand is very fine to coarse skewed (-0.54 to 2.85 ϕ) and mesokurtic to very leptokurtic (2.6 to 8.13 ϕ). The sand from this lithofacies contains mud-sized grains, and they represent ~ 4% of the total sediments. The majority of grains (~80%) from this sand tend to be angular to sub-angular in shape, and the other grains are sub-rounded. Approximately, 70% of the grains have low sphericity and 30% of the grains have high sphericity. The sand from this lithofacies is texturally submature to mature.

The lithofacies contains some burrows that are ~2-8 cm long (Fig. 20). Color mottling is also present widely within this lithofacies, especially in section 2 (Fig. 18). Mud clasts ~0.5-2 cm thick and 1-2 cm wide are also present in this lithofacies (Fig. 19). This lithofacies is mostly

massively bedded, but low angle cross-bedding can be seen in some beds in section 2. In section

5, this lithofacies alternates with lithofacies 7 and 8, and in section 2, it is overlain by lithofacies

3 with a sharp contact.

Figure 17. Sand lenses (red arrows) in lithofacies 3. Vertical gouges are the result of excavator bucket teeth digging out this exposure.
.

Figure 18. Lithofacies 5. Color Mottling (blue arrows) and mud clasts (red arrows) in lithofacies 5. A 28-cm-long spade for scale.

Figure 19. Mud clasts (red arrows) in lithofacies 5. A 19-cm-long pencil for scale.

Figure 20. Burrows (red arrows) within lithofacies 5.

Lithofacies 6

This lithofacies is composed of orange to light gray medium sand. The lithofacies is present in sections 1 and 2, and its thickness ranges from 0.25 to 0.85 m. The mean grain size of sand is 1.94 ϕ, while the maximum grain size is >1 ϕ. The standard deviation of this sand is 0.67 ϕ, classifying it as moderately well sorted (Folk, 1980). It has skewness values of 0.66 to 1.09 ϕ (fine skewed) and kurtosis values of 0.94 and 4.89 ϕ (very platykurtic to leptokurtic). Approximately 80% of sand grains are angular to sub-angular, and 20% are sub-rounded. Highly spherical grains make up ~70% of the total grains in the observed sample, whereas the others have low sphericity. The sand in this lithofacies has a low proportion of mud-sized materials that do not exceed 2% of the total grains. Texturally, the sand is submature to mature.

This lithofacies contains mud lenses that vary in thickness from a few millimeters to a few centimeters (Fig. 21). Also, there are undulatory mud drapes present within the sand beds (Fig. 21). Some beds also contain herringbone cross stratification (Fig. 21), and low to medium angle cross-bedding (Fig. 22). This lithofacies is overlain by lithofacies 9 via a gradational contact.

Lithofacies 7

This lithofacies consists mainly of medium-bedded (up to 25 cm thick) light to dark brown medium sandstone. The lithofacies is exposed in the lower part of section 5. The sandstone has an average grain size of 1.4 ɸ and a maximum grain size of >0.25 ɸ. The sandstone is moderately sorted and has a standard deviation value of 0.71 ɸ. The sandstone is fine skewed (0.82 ɸ) and platykurtic (2.05 ɸ). Mud-sized grains in this sandstone make up ~2% of the total sediment. The sandstone in this lithofacies has 60% sub-angular grains, 30% angular grains, and 10% sub-rounded grains. Low sphericity grains represent 65% of the total grains, whereas the highly spherical grains make up 35%.

The lithofacies is massively bedded and is intensely bioturbated with Fe-cemented burrows. The lithofacies is only present in section 5, where it is overlain by lithofacies 5 with a sharp contact.

Figure 21. Sand in lithofacies 6 containing mud drapes (red arrows) and herringbone cross-stratification (blue arrows). A16-cm-long pen for scale.

Figure 22. Cross laminations (black arrow) and mud lens (red arrow) in lithofacies 6. A 19 cm-long field book for scale.

.

Lithofacies 8

This lithofacies consists of medium- to thick-bedded (0.3-0.5 m), dark brown, coarse sandstone. The lithofacies is present within section 5. The average grain-size of this lithofacies is 0.4 ɸ, while the maximum grain-size is -0.8 ɸ. The sandstone has a standard deviation value that

ranges from 1.09 to 1.34 φ, indicating poor sorting (Folk, 1980). The sandstone has a skewness

of 1.52 to 2.73 φ (very fine skewed) and kurtosis of 2.72 to 6.73 φ (mesokurtic to leptokurtic).

The matrix does not exceed 1.5% of the total rock sample observed. The roundness of grains

varies, with 20% angular, 65% sub-angular, 10% sub-rounded, and 5% rounded. The majority of

the grains (~75%) are highly spherical, while the others have low sphericity. The sandstone is

texturally immature to submature.

The lithofacies is massively bedded and is characterized by Fe-cemented burrows that

have a diameter of 1-3 cm (Fig. 23). The Fe cementation obscures details of many of the

burrows, but well-preserved examples appear to be *Ophiomorpha*. This lithofacies also contains

irregular, concentric iron concretions containing vugs that range in size from 1 cm to several

centimeters (Fig. 24). Lithofacies 8 is underlain by lithofacies 5 via a sharp contact.

Lithofacies 9

This lithofacies is composed of laminated gray mud. Beds range in thickness from 20 to

25 cm and are present in sections 1 and 2. The mud has standard deviation values of 0.25 to

0.44 φ, showing well to very well-sorted grains. It has a negative skewness of -3.38 to -1.03 φ

(very coarse to coarse skewed) and kurtosis values of 2.11 and 12.56 φ (platykurtic and very

leptokurtic).

The lithofacies contains parallel lamination and sand lenses that range from 0.5-2 cm in

thickness. This lithofacies is overlain by lithofacies 1 in section 1 and lithofacies 5 in section 2

with sharp contacts.
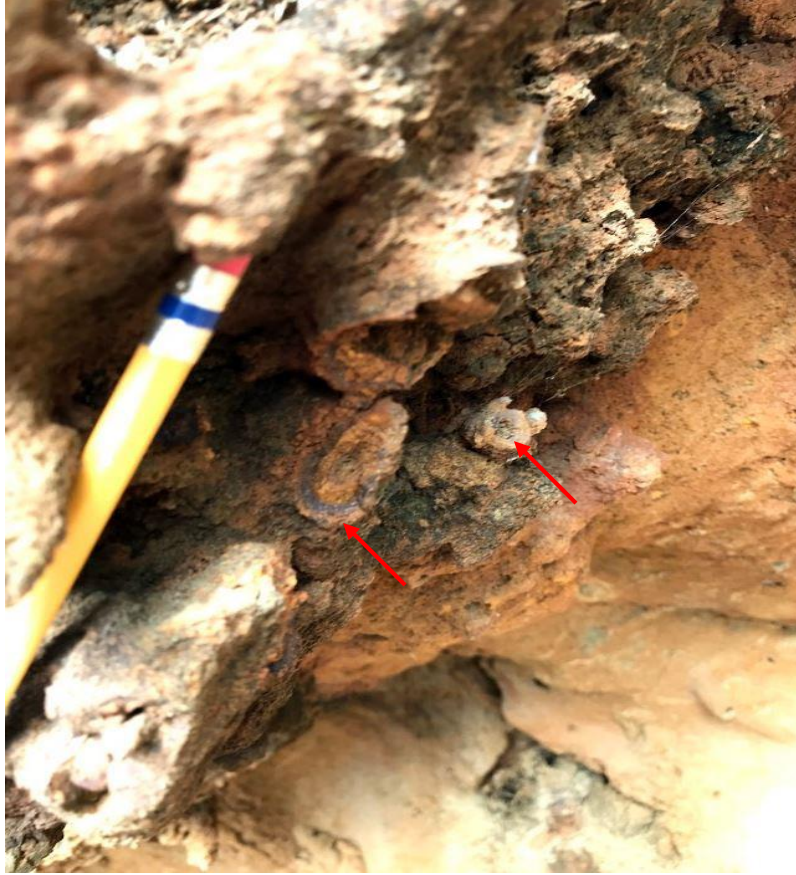
Figure 23. Fe-cemented burrows (red arrows) in lithofacies 8. An 18-cm-long pencil for scale.

Figure 24. Vugs are shown by red arrows in lithofacies 8. A 28-cm-long spade for scale.

Table 2. Grain-size data, desecription and interpretation of the 9 lithofacies from the Meridian Sand.

Lithofacies Number	Sample ID	Mean grain-size (ϕ)	Mean grain-size term	Standard deviation (ϕ)	Skewness	Kurtosis	Sorting	Description	Interpretation
1	M3-01 M3-02 M4-01	3.16	Very fine sand	0.8	0.31	2.4	Moderately sorted	Light gray to light yellow massive sand. Contains mud clasts and burrows.	Lower subtidal to foreshore setting.
2	M1-01	3.03	Very fine sand	1.31	0.08	0.14	Poorly sorted	Light gray massive sand. Contains mud clasts and burrows.	Intertidal environment (sand flat).
3	M1-04, M2-06	3.43	Very fine sand	0.87	0.45	2	Moderately sorted	Light gray muddy sand. Contains wave ripples and orange sand lenses.	Intertidal (mixing flat) environment.
4	M1-05, M1-06, M4-02	2.65	Fine sand	0.64	0.57	5	Moderately well sorted	Light yellow to orange massive sand interbedded with thin mud beds.	Subtidal to intertidal (sand flat and mixing flat) environment.
5	M2-01, M2-03, M2-04, M2-05, M5-01, M5-03, M5-05	2.54	Fine sand	0.76	0.95	4.54	Moderately sorted	Light gray to orange sand and sandston. Mud clasts and burrows are present.	Subtidal to lower intertidal (sand flat) environment.
6	M1-02, M3-03	1.94	Medium sand	0.67	0.87	2.93	Moderately well sorted	Orange to gray sand. Contains mud lenses, mud drapes, cross-bedding, and herringbone cross-stratification.	Intertidal (mixing flat) environment.
7	M5-02	1.4	Medium sand	0.71	0.82	2.05	Moderately sorted	Medium-bedded light to dark brown sandstone.	Lower intertidal (sand flat) setting.

								Contains Fe-cemented burrows.	
8	M5-04, M5-06	0.4	Coarse sand	1.26	2.12	7	Poorly sorted	Medium-to thick-bedded dark brown sandstone. Massively bedded and characterized by Fe-cemented *ophiomorpha* burrows.	High energy shoreface setting (upper shoreface).
9	M1-03, M2-02	4.33	Mud	0.34	-2.20	7.33	Very well sorted	Laminated gray mud. Orange sand lenses are present.	Intertidal mud flat setting.

Petrography

Modal analysis

The results of the petrographic study for sand and sandstone samples are provided in Table 3. Photomicrographs for sand and sandstone samples can be seen in Fig. 25. Four hundred grains were identified from sand and sandstone samples based on the technique of Dickenson & Suczek (1979), which includes grains that are larger than 63.5 μm.

Quartz is the most abundant mineral in all sand and sandstone samples studied, accounting for more than 90% of the total framework grains. Sample M1-02 from lithofacies 2 has the highest percent of quartz (97.8%) and sample M4-02 from lithofacies 4 has the lowest percent of quartz (88%). Quartz grains range in size from very fine to coarse and they are dominantly angular to sub-angular. Quartz occurs as both monocrystalline and polycrystalline grains only in 8 samples collected from sections 1 and 2, while the other samples contain only monocrystalline quartz grains (Fig. 25). The percentage of monocrystalline grains range from 93.7 to 100% with an average of 99.2% of the total quartz grains. Polycrystalline quartz grains (Fig. 25B) are much less abundant than monocrystalline quartz grains, and were only identified in 8 samples. The proportion of polycrystalline quartz ranges from 0.27 to 4.34% of the total quartz grains. Polycrystalline grains are mostly fine to medium, and sub-angular to sub-rounded.

Lithic fragments are the second most abundant grain type in all sand and sandstone samples and they make ~4% of the total sand grains. The only types of lithic grains present are sedimentary; no volcanic or metamorphic grains were identified. The percentage of sedimentary lithics ranges from 0.3 to 10.8% with an average of 4.08%. Samples M3-01 from lithofacies 1 and M4-02 from lithofacies 4 have the lowest percentage of quartz (<90%) and have the highest

proportion of sedimentary lithics (10.8 and 10%, respectively). Sedimentary lithics range in size from very fine to coarse sand, and they are sub-angular to sub-rounded. Sedimentary lithics include shale fragments and chert (Figs. 25C & 25E). Shale fragments are the most abundant lithic, and they account for more than 3% of the total sand grains and 74.4% of total lithics. Chert grains are less abundant than shale fragments, and they make up less than 1% of the total framework grains and 25.6% of total rock fragments.

Feldspar grains are found in minor amounts within the Meridian Sand in the study area. The percentage of feldspar ranges from 0. 3 to 1%, with an average percentage of 0.3%. Both plagioclase and K-feldspar are present (Figs. 25D & 25H). Plagioclase accounts for 44.8% of the total feldspar grains, whereas K-feldspar accounts for 55.2% of the total feldspars. Feldspar grains vary in size from very fine to medium, and they are angular to sub-angular in shape.

Micas make up 0.3 to 6.2% of the total grains in all samples, except samples M3-03 from lithofacies 6 and M5-01 from lithofacies 5, which are poor in micas. Sample M1-04 from lithofacies 3 has the highest percent of mica: 6.2% of the total sand grains. Muscovite and biotite are both present (Figs. 25A & 25F). Muscovite is the most abundant mica, accounting for more than 1% of the total sands and 99.5% of the total mica grains. Muscovite grains are mainly elongated in shape and their size ranges from very fine to medium. Biotite is found in minor amounts in samples M2-03, M2-04, M2-05. They are very fine to fine in size, and they are mostly sub-angular.

Heavy minerals including zircon and magnetite make up ~0.4% of the total composition of sand and sandstone. Zircon is found only in 6 samples where it ranges from 0.2 to 0.7% of the total composition. Zircons are very fine in size and have high relief (Fig. 25A). Magnetite is more abundant than zircon and in some samples it makes up more than 1% of the total sand

volume. It is found in all samples, and it ranges from 0.2 to 1.5%. The magnetite grains are very

fine to fine in size, sub-angular to angular in shape, and they are opaque under crossed and

plane-polarized light (Fig. 25I).
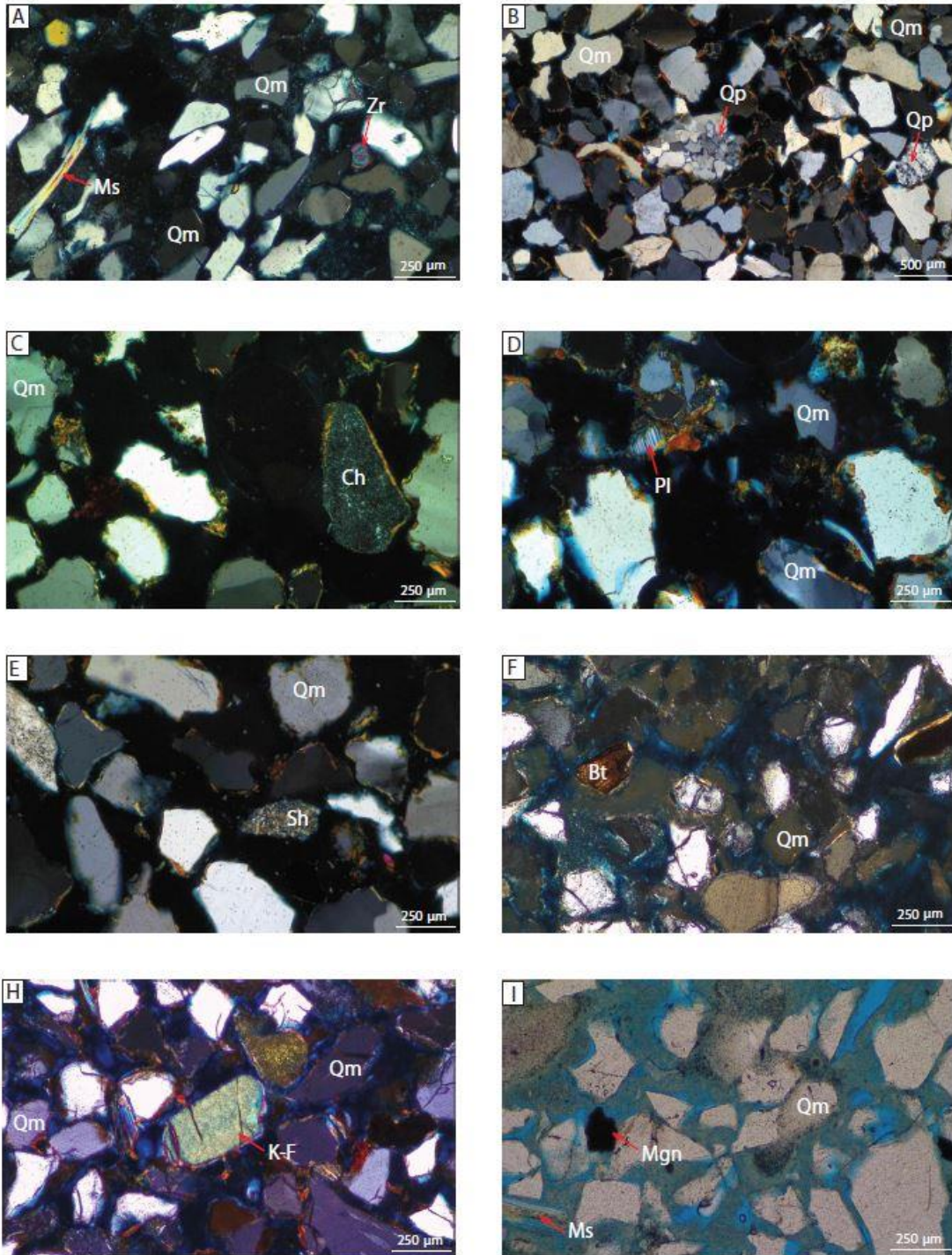
Figure 25. Photomicrographs of sand and sandstone samples. Qm: monocrystalline quartz; Qp: polycrystalline quartz; Pl: plagioclase; K-f: k-feldspar; Ms: muscovite; Bt: biotite; Zr: zircon; Mgn: magnetite; Sh: shale fragment; Ch: chert. Images A, B, C, D, H under crossed polarized light; F and I under plane-polarized light.

50

Diagenetic features

Cement is present in a few sand and sandstone samples. Two types of cement were determined based on petrographic properties: hematite and clay cements. Hematite cement can be seen clearly in sample M1-02 from lithofacies 6, and samples M1-05, and M1-06 from lithofacies 4, where it mostly coats all grains, and in same parts, it connects sand grains (Fig 26D & 26F). Hematite cement can also be seen in sample M2-03 from lithofacies 5, coating some sand grains (Fig. 26C).

Clay cement is present in sample M2-03. The clay cement is filling pore space and it is distinguished by a cloudy greenish appearance (Fig. 26C). Clay cement can also be seen in sample M1-01 from lithofacies 2, where cement fills some of the pore spaces. A second type of clay cement, which is distinguished by its brown color, was observed in some samples. This cement tends to coat the edges of grains and connects some grains (Fig. 26A).

Some well-cemented sandstones contain possible hydrocarbon staining that fills almost all the pore space. Some hematite cement can be seen along the boundaries of some quartz grains where the staining is present (Fig.26E). Due to the staining of hydrocarbon that fills the pore space (Fig. 26E), it is difficult to see if there are other cements filling the spaces between grains.

Other diagenetic features include dissolution and fracturing of grains. These features are only observed in a few samples (Figs. 27C & 27D). Most of these sand grains are not in contact except two samples (M2-05 and M3-01), which show point to point contacts (Fig. 27A). Other diagenetic features include bending of muscovite grains, which is seen in two samples (M2-06 from lithofacies 3, M3-03 from lithofacies 6), (Fig. 27B).
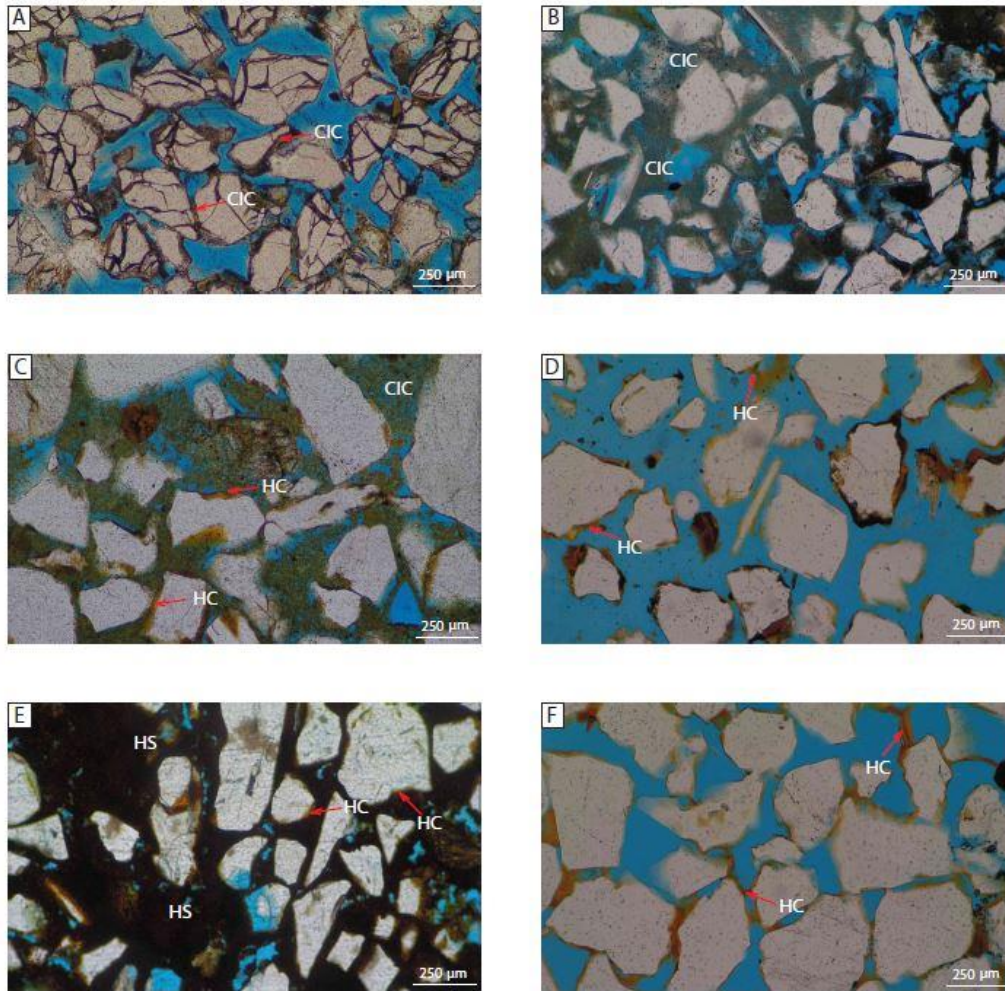
Figure 26. Photomicrographs of sand and sandstone samples from the Meridian Sand showing cement types. ClC: clay cement; HC: hematite cement; Hs: hydrocarbon staining. All images are under plane-polarized light.
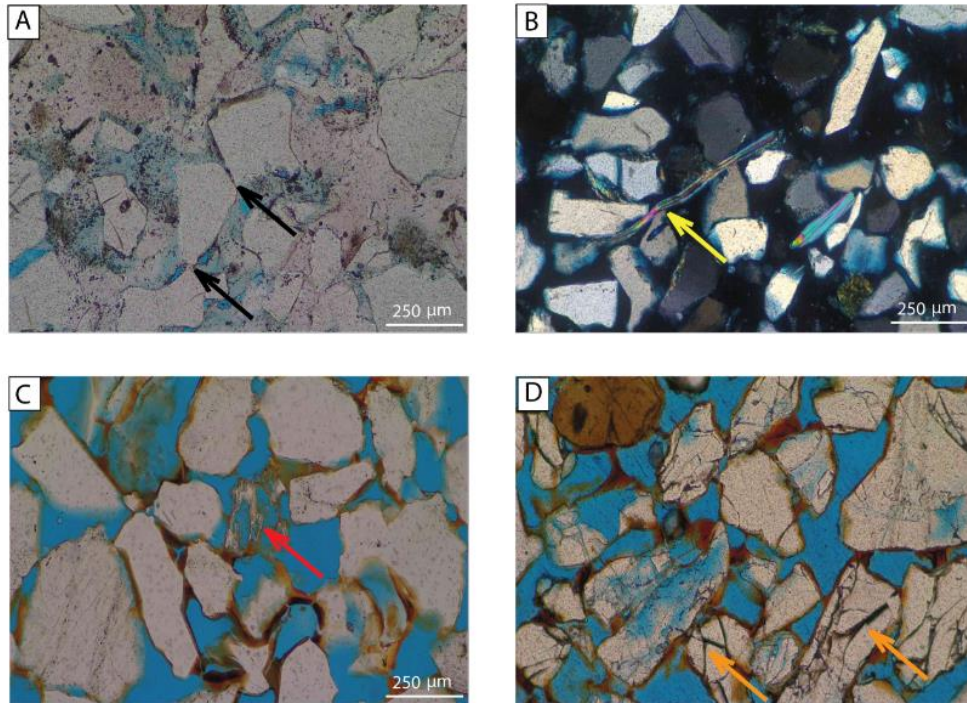
Figure 27. Photomicrographs of sand and sandstone samples showing diagenetic features. A, B and C are under plane-polarized light, and B is under crossed-polarized light. Red arrow shows quartz dissolution; black arrows show point to point contacts; yellow arrow shows bent muscovite grains; orange arrows show fracturing of quartz grains.

Sand and sandstone classification

Dott's (1964) classification was used in this study to classify sand and sandstone samples from the Meridian Sand Member. In this classification, two criteria are used to subdivide sands and sandstones: relative percent of matrix (mud-sized grains) and relative abundances of quartz, feldspar, and rock fragments. Sands and sandstone with < 15% matrix are classified as arenites, whereas samples with a higher proportion of matrix (>15-50%) are classified as wackes. The percentages of quartz, feldspar, and lithics are used to subdivide arenites and wackes. Arenite is subdivided into five categories: 1, quartz arenite (>95% quartz); 2, sublitharenite (75-95% quartz and lithics > feldspars); 3, subarkose (75-95% quartz and feldspars > lithics; 4, lithic arenite (75-100% lithics), and arkosic arenite (75-100% feldspars). Wackes are grouped into three categories: quartzwacke (> 95% quartz); lithic greywacke (< 95% quartz and lithics > feldspars); feldspathic greywacke (> 95% quartz and feldspars > lithics) (Dott, 1964).

According to Dott's (1964) classification, the Meridian Sand samples from Grenada County are classified as quartz arenites, sublitharenites, quartz wackes, and lithic graywackes (Figs 28 & 29). Quartzarenite is the most dominant sand and sandstone type (10 samples), and it is dominant in sections 1 and 2. Sublitharenite (8 samples) is more dominant in sections 3, 4, and 5. Only three samples (M1-04, M2-06, M4-01) are classified as quartzwackes, and samples M3-01 and M3-02 are classified as lithic graywackes.
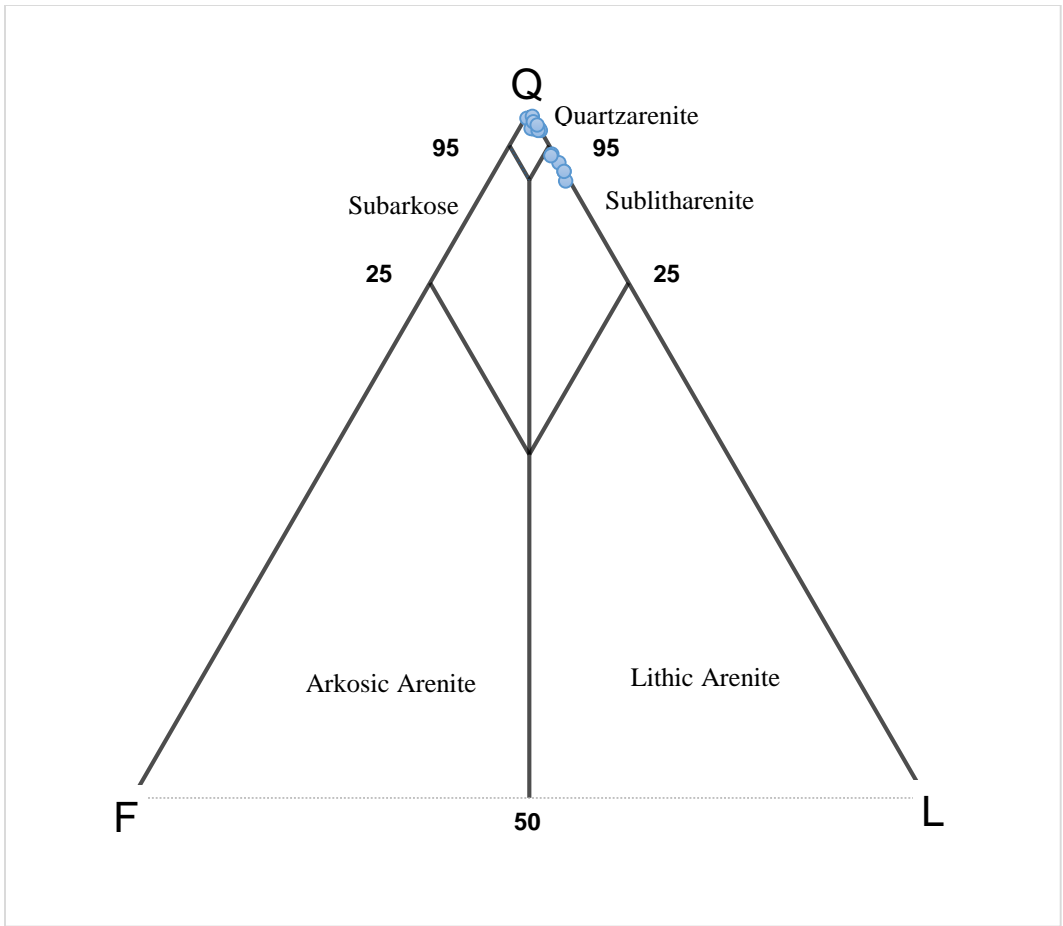
Figure 28. Dott (1964) classification of Meridian Sand samples with 0 to < 15% matrix.
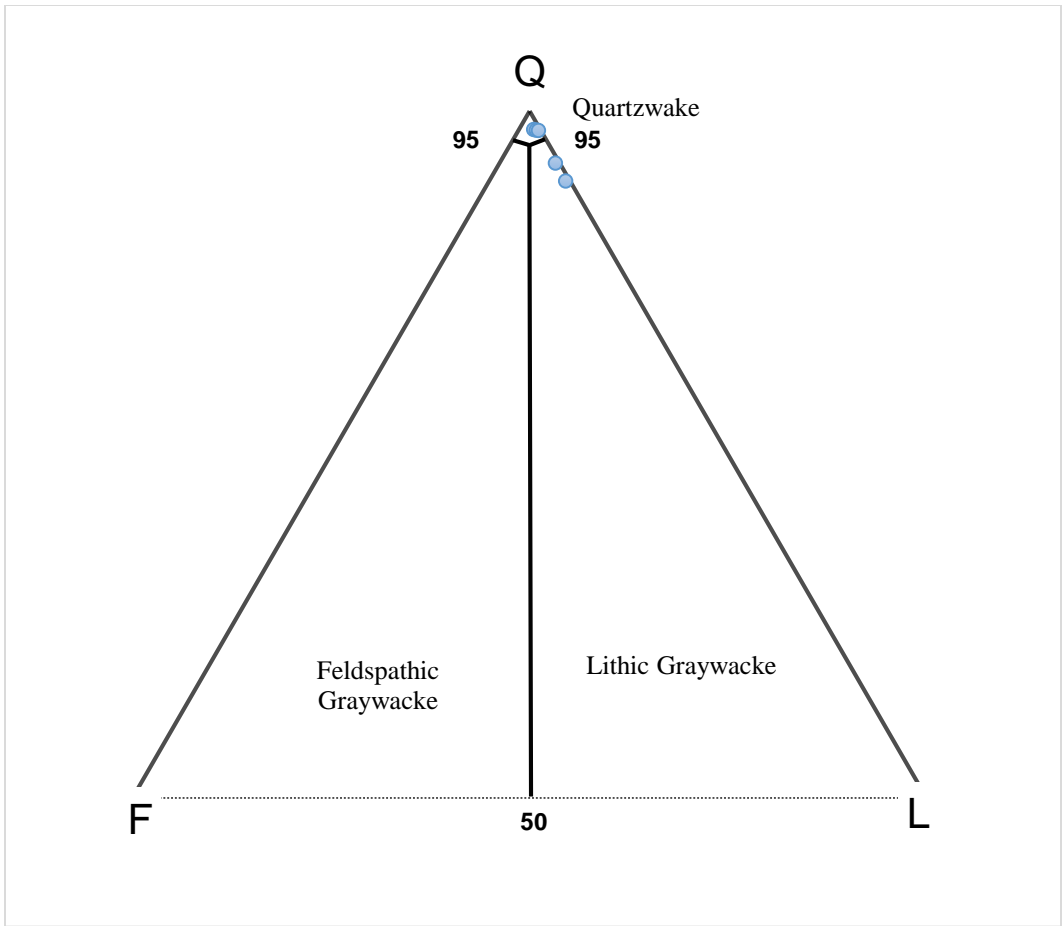
Figure 29 Dott (1964) classification of Meridian Sand samples with 15 to 50% matrix.

Table 3. Mineralogical composition of sand and sandstone samples from the Meridian Sand. Qt: total quartz; Qm: monocrystalline quartz; Qp: polycrystalline quartz; Ft: total feldspar; Pl: plagioclase; K-f: potassium feldspar; Lst: sedimentary lithic; Sf: shale fragment; Che: Chert; Mit: total mica; Ms: muscovite; Bt: biotite; Zr: zircon; Mgn: magnetite.

Sample No	Qt	Qm	Qp	Ft	Pl	K-f	Lst	Sf	Che	Mit	Ms	Bt	Zr	Mgn	Q:f:L	Pl: K-f	Qm: Qp
M1-01	94.5	93.5	1.25	0.5	0	0.5	1.75	1.75	0	1.5	1.5	0	0.25	1.5	97.42:0.77:1.8	0:100	98.62:1.32
M1-02	97.75	93.5	4.25	0.5	0.25	0.25	0.75	0.5	0.25	0.75	0.75	0	0	0.25	98.98:0.25:0.75	50:50	95.65:4.34
M1-04	92.25	91.75	0.5	0	0	0	1.5	1.5	0	6.25	6.25	0	0	0	98.4:0:1.6	-	99.45:0.54
M1-05	95.25	89.25	6	0.75	0	0.75	0.25	0	0.25	1.25	1.25	0	0	0.5	98.96:0.77:0.258	0:100	93.7:6.3
M1-06	93	92.5	3.5	1	0.75	0.25	1.5	0.75	0.75	0.75	0.75	0	0.75	0	97.46:1.01:1.52	75:25	96.35:3.65
M2-01	94.5	94.25	0.25	0	0	0	3	3	0	0.5	0.5	0	0	0	97.42:0:2.57	-	99.73:0.27
M2-03	94	95.5	0	0	0	0	0.75	0.75	0	2	1.75	0.25	0	1.25	99.2:0:0.79	-	100:0
M2-04	95.5	94.75	0.75	0	0	0	2.75	0.75	2	1.5	1.25	0.25	0	0.25	97.2:0:2.79	-	99.21:0.79
M2-05	95.25	94.75	0.5	0.25	0.25	0	1.25	1	0.25	2.25	2	0.25	0.25	0.75	98.44:0.25:1.29	100:0	99.47:0.53
M2-06	95	95	0	0	0	0	1.5	0.75	0.75	2.5	2.5	0	0	1	98.7:0:1.29	-	100:0
M3-01	88.25	88.25	0	0	0	0	10.75	8	2.75	0.25	0.25	0	0	0.25	89.14:0:10.85	-	100:0
M3-02	91.75	91.75	0	0.5	0.25	0.25	7	5	2	0.75	0.75	0	0	0	92.44:0..5:7.05	50:50	100:0
M3-03	97	97	0	0.5	0	0.5	2.25	2.25	0	0	0	0	0.25	0	97.24:0.5:2.25	0:100	100:0
M4-01	95.5	95.5	0	0.25	0.25	0	2.5	2.5	0	1.25	1.25	0	0.25	0.25	97.20:0.25:2.54	50:50	100:0
M4-02	88	88	0	0.5	0.25	0.25	10	9.5	0.5	1	1	0	0	0.5	89.79:9.69:0.51	50:50	100:0
M5-01	93.75	93.75	0	0.25	0.25	0	6	6	5	0	0	0	0	0	93.75:0.25:6	100:0	100:0
M5-02	92.25	92.25	0	0.5	0.5	0	7.5	7	0.5	0.25	0.25	0	0	0	92.48:0:7.52	-	100:0
M5-03	90.75	90.75	0	0	0	0	8.75	8.75	0	0.25	0.25	0	0	0.25	91.2:0:8.80	-	100:0

M5-04	93.5	93.5	0	0.5	0.5	0	5.75	5.75	0	0.25	0.25	0	0	0	93.5:0.5:6	100:0	100:0
M5-05	96.5	96.5	0	0	0	0	2	2	0	0.25	0.25	0	0.25	0.5	97.96:0:2.03	-	100:0
M5-06	91	91	0	0	0	0	8.75	8.25	0.5	0.25	0.25	0	0	0	91.22:0:8.77	-	100:0

X-ray fluorescence(XRF) analyses

Major oxides (SiO_2, Al_2O_3)

SiO_2 is the most abundant oxide in the sand and sandstone samples with an average value of 84.2%. Most sand and sandstone samples have high to moderate SiO_2 concentrations that range from 76.1 to 95.5% (Fig. 30). Only two samples have lower values of SiO_2: 47.9% for sample M5-06; and 68.3% for sample M5-04. (Fig. 30). There is no relationship between the values of SiO_2 and the stratigraphic positions of the collected samples (Fig. 30). In mud samples (M1-03, M2-01), the SiO_2 values are 89.5%, and 85.3%, respectively.

Al_2O_3 concentrations are low in comparison to SiO_2 concentrations. Al_2O_3 values range from 2.5 to 14.5% in all samples (Fig. 31), except sample M5-06, which has the highest concentration of Al_2O_3 at 16.2% (Fig. 31). The average value of Al_2O_3 in all samples is 7.7%. Al_2O_3 values do not show any relation with the stratigraphic position or sample lithology. SiO_2/Al_2O_3 ratios tend to be high in most samples, ranging from >6 to 37.5%. Only two samples show low SiO_2/Al_2O_3 ratios: 5.7% for sample M5-03; and 3.2% for sample M5-06.
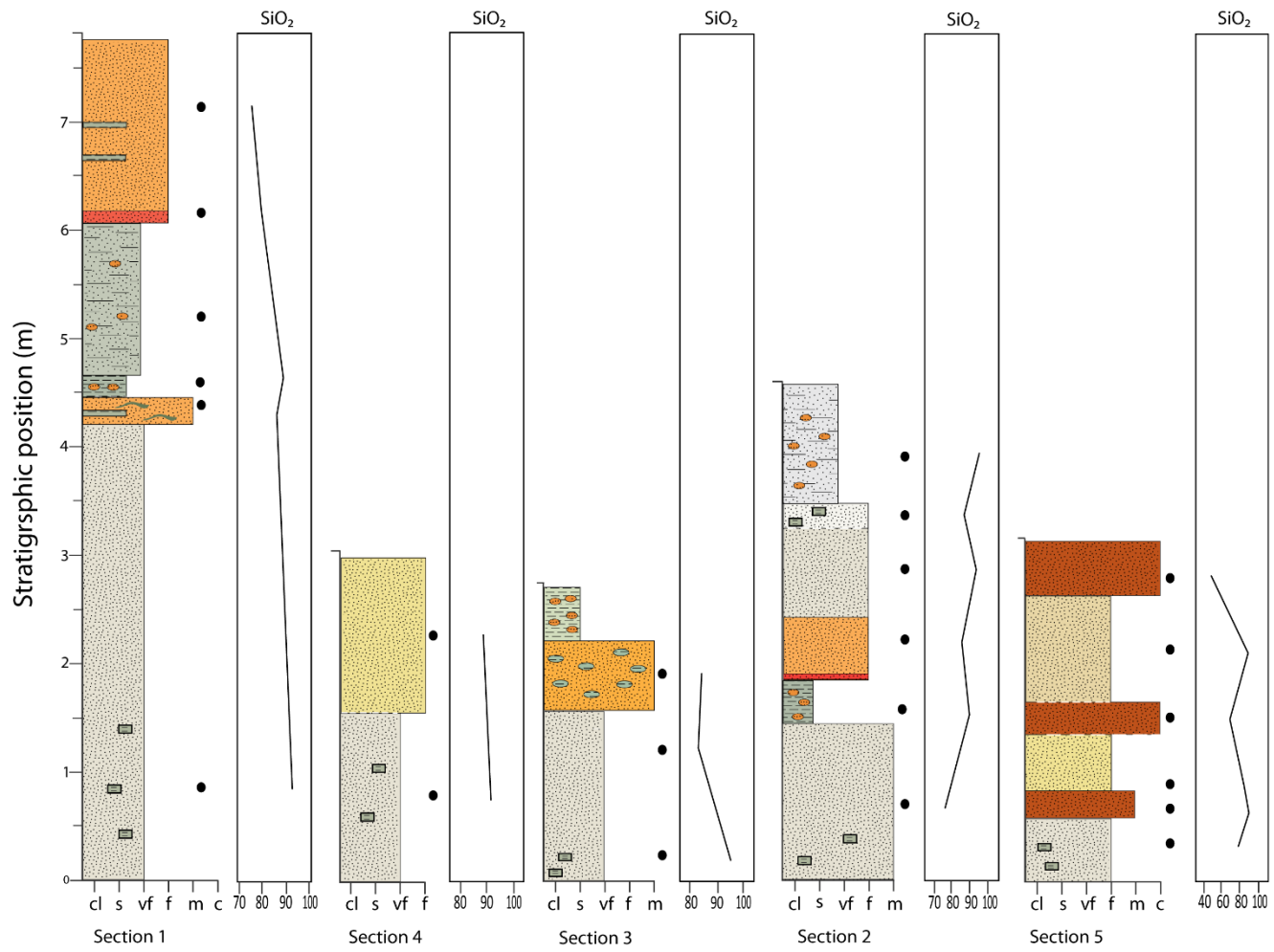
Figure 30. Stratigraphic columns of the five sections showing SiO_2% values of collected samples.
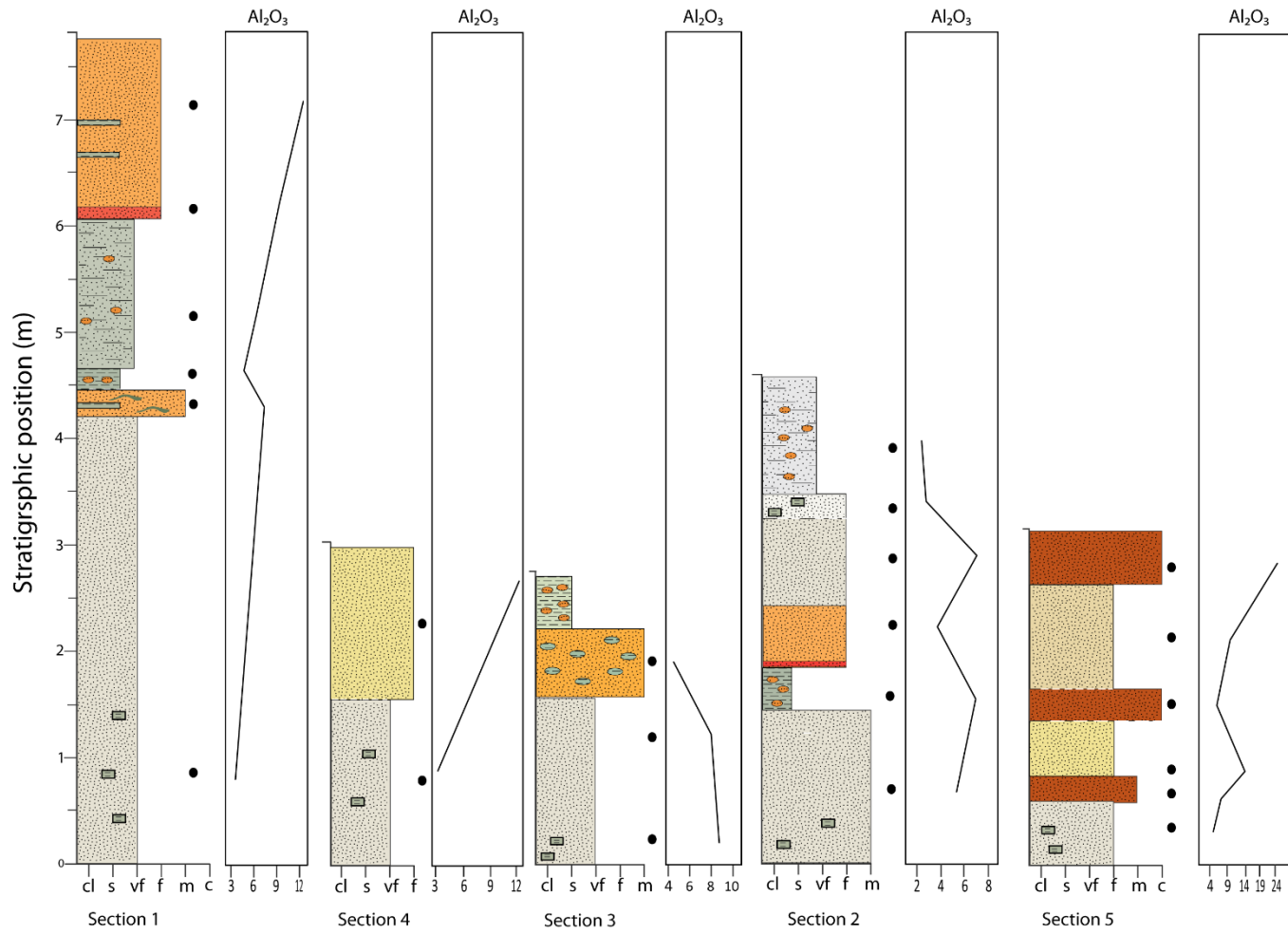
Figure 31. Stratigraphic columns of the five sections showing Al$_2$O$_3$% values of collected samples.

Trace elements

The most useful trace elements for provenance interpretations are scandium (Sc), thorium (Th), and zirconium (Zr). These elements are found in minor amounts within the Meridian Sand. Zr is the dominant trace element among the three, with an average of 318.6 ppm. The majority of Zr values are below 800 ppm, and they range between 66.07 and 760.09 ppm. Sample M1-03 has the highest concentration of Zr with 874.45 ppm. Sc and Th values in comparison to Zr values are very low, and they both are below 100 ppm. The average values of Sc and Th concentrations are 1.67 and 5.92 ppm, respectively. Samples M1-03 and M1-04 have the highest concentration of Th, with values of 13.01 and 13.63 ppm, respectively. A ZrScTh ternary diagram (Fig. 32) shows that all data plot at the top of the diagram due to zirconium enrichment.
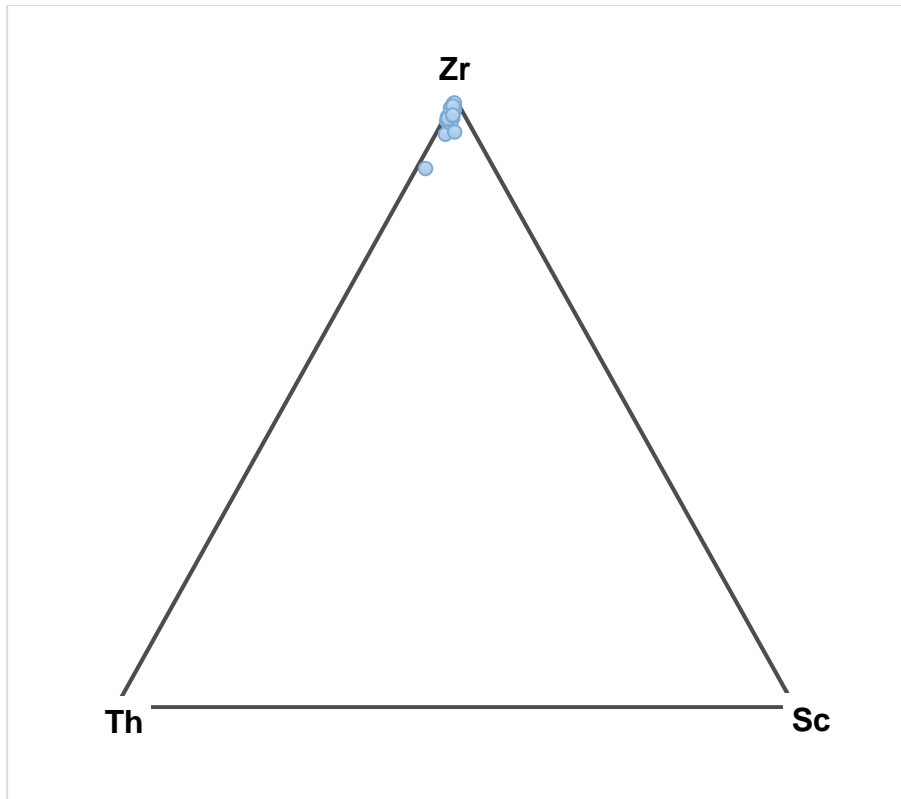
Figure 32 Ternary diagram showing relative abundances of Zr, Sc, and Th in all 23 samples.

X-ray diffraction (XRD) analyses

XRD analyses were performed to determine the mineralogical composition of two mud-dominated samples (M1-03, M2-02), which had grains too small to point count in thin section. The samples were collected from sections 1 and 2. Results showed the presence of quartz, zeolites, clays, and micas. Quartz is found in both samples and makes up ~ 36% of sample M1-03, and 54.9% of sample M2-02 (Fig. 33). Tridymite, which is a polymorph of quartz is found only in sample M1-03, and is less abundant than quartz, making up ~31.3% of the total minerals in this sample. Clay minerals make up ~19.88% of the total minerals in both samples. The clay minerals are nacrite and dickite; both polymorphs of kaolinite. Dickite concentrations vary in both samples, and are higher in sample M2-02 (~18.5%), whereas in sample M1-03, dickite makes up ~6.3% (Fig. 33). Nacrite is only present in sample M1-03, where it is less abundant than quartz and tridymite, and it is more abundant than dickite. The nacrite concentrations in this sample are 15.0% (Fig. 33). Muscovite is present only in sample M1-03, and it represents 10.7% of the total mineral composition of this sample. Laumontite, a zeolite, is the second most abundant mineral in sample M2-02, and it makes up ~26.7% of the total composition (Fig. 33).
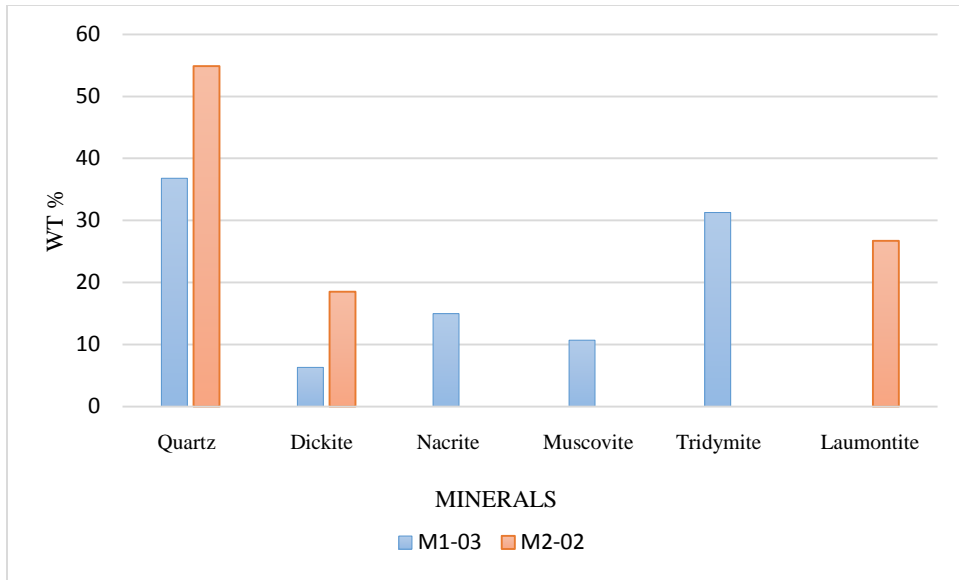
Figure 33. The mineralogical composition of two mud-dominated samples from the Meridian Sand.

DISCUSSION

Provenance and parent rock interpretation

Sand and sandstone provenance

The composition of the source area has major control on the mineral composition of sandstones. Other controls of sandstone composition include transport mechanism, climate, and diagenesis (Dickenson et al., 1983). The mineral abundances calculated from point counting were used to interpret provenance and tectonic setting of sandstones (Dickinson, 1985). Dickenson (1985) defined three provenance categories; continental block, magmatic arc, and recycled orogen. Continental block describes tectonically integrated regions composed of eroded, ancient orogenic belts. Magmatic arc is defined as belts composed mainly of associations of plutonic and volcanic rocks with metamorphic rocks generated along arc-trench systems. Recycled orogens are composed of uplifted and deformed supracrustal rocks, mainly sedimentary, but also some volcanic rocks, formed in orogenic regions (Dickinson, 1985).

Results of modal analyses of sand and sandstone samples were plotted on a QtFL ternary diagram of Dickenson (1985) (Fig. 34). Thirteen samples (quartzarenites and quartzwackes) fall in the continental block provenance (craton interior). The craton interior is composed of felsic granitic rocks, metamorphic rocks, and successions of sedimentary rocks (Dickenson, 1985). The high content of quartz and the high Qm/Qp ratios in all these quartzarenites and quartzwackes reflects the greater potential of stable monocrystalline quartzes to survive in the sedimentary

cycle (Folk, 1975). According to Dickenson (1985, 1983), sandstones derived from stable cratons are deposited in local basins associated with the craton and foreland basins. The majority of grains in quartzarenites and quartzwackes are angular to sub-angular, supporting the interpretation that these rocks were likely deposited near to the source region.

Eight samples fall in the recycled orogenic field in the QtFL diagram (Fig. 34), and all of these samples are either sublitharenites or lithicgraywackes. These samples fall in the recycled orogenic field because their quartz content is less than 95% and they have high sedimentary lithic content relative to feldspar content. According to Dickenson (1985), sandstones derived from the recycled orogen province (subduction complex or fold-thrust belt) are low in feldspars and volcanic lithics. Furthermore, these recycled orogens are composed of sedimentary or metasedimentary rocks (Dickenson & Suczek, 1979). Recycled orogenic is a possible source for sublitharenites and lithicgraywackes of the Meridian Sand because of their low feldspar content. Also, they are poor in volcanic and metamorphic lithics and rich in sedimentary lithics. The craton interior is the only provenance indicated for all sand and sandstone samples from the Meridian Sand on the QmFLt ternary diagram (Fig. 35) because all samples are rich in monocrystalline quartz. In the QmFLt ternary diagram, samples do not fall in the recycled orogenic field because lithics and polycrystalline quartz grains make up <10% of the framework grain population, so most samples fall only at the top of the QmFLt ternary diagram.

All samples fall at the top of the QmPK ternary diagram (Fig. 36). This indicates an increase in stability and mineralogical maturity of sand and sandstones. The reason that all samples fall at the top of the diagram is because they are rich in monocrystalline quartz in comparison to feldspar (K-feldspar and plagioclase).

The QpLvLs ternary diagram shows that sand and sandstones were derived from collision orogen sources due to their high content of sedimentary lithics relative to polycrystalline quartz. Sandstones with high Ls/Lv ratios can be indicators of collision orogens (Dickenson, 1983; Dickenson, 1985). This supports the QpLvLs ternary diagram (Fig. 37), which shows high Ls/Lv ratios. The presence of sedimentary fragments such as shale and chert might be an indication of a recycled sedimentary source (Dickenson, 1985).

The Meridian Sand is interpreted to be sourced from craton interior and recycled orogenic provinces, however, the geographic locations of the source regions need to be determined. Previous studies (e.g., Grim, 1936; William et al., 2013) focused on the provenance of the Eocene Claiborne Group in Mississippi and Texas. However, there has not been much specific research either on the provenance of the Meridian Sand or the Tallahatta Formation. Grim (1936) used assemblages of detrital zircons to interpret the provenance of Claiborne Group. He defined the geographic location of the provenance to be the southern portion of the Appalachian region. Other studies (e.g., Chen, 1965; Galloway, 1968) show that the southern Appalachians were an important source of Paleogene and Neogene sediments. William et al. (2013) agree with Grim (1936) that Claiborne Group sediments in the ME were derived from the Appalachians, and this was based on detrital zircon dating. Grim (1936) stated that Claiborne Group sediments might have been sourced from two different geographic locations based on the differences in grain shape. He interpreted the rounded zircon grains to have undergone recycling, while a population of angular grains might have come directly from the parent rock. In Grenada County, most of the zircons are fine-sand sized with rounded shapes (e.g., Fig. 25A). The properties of these rounded zircon grains are consistent with those described as recycled by Grim (1936) and they might have been derived from the southern Appalachians.

Although angular zircon grains were not observed in the Grenada County samples, a subset of the samples is characterized by angular to sub-angular framework grains, supporting the hypothesis that a secondary, proximal source contributed to the Meridian Sand. This agrees with Grim's (1936) interpretation of a secondary nearby source of Claiborne sediment.
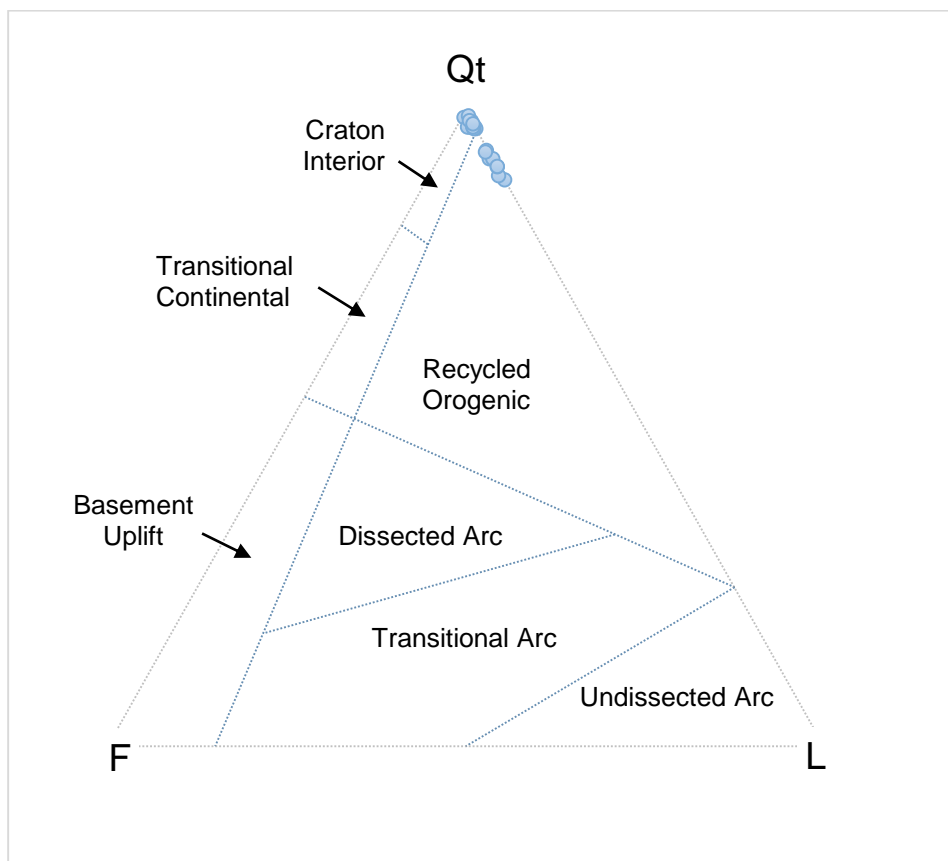
Figure 34. QtFL ternary diagram (Dickenson, 1985) of framework mineralogy for the Meridian Sand showing that sands and sandstones fall in the craton interior and recycled orogenic fields.
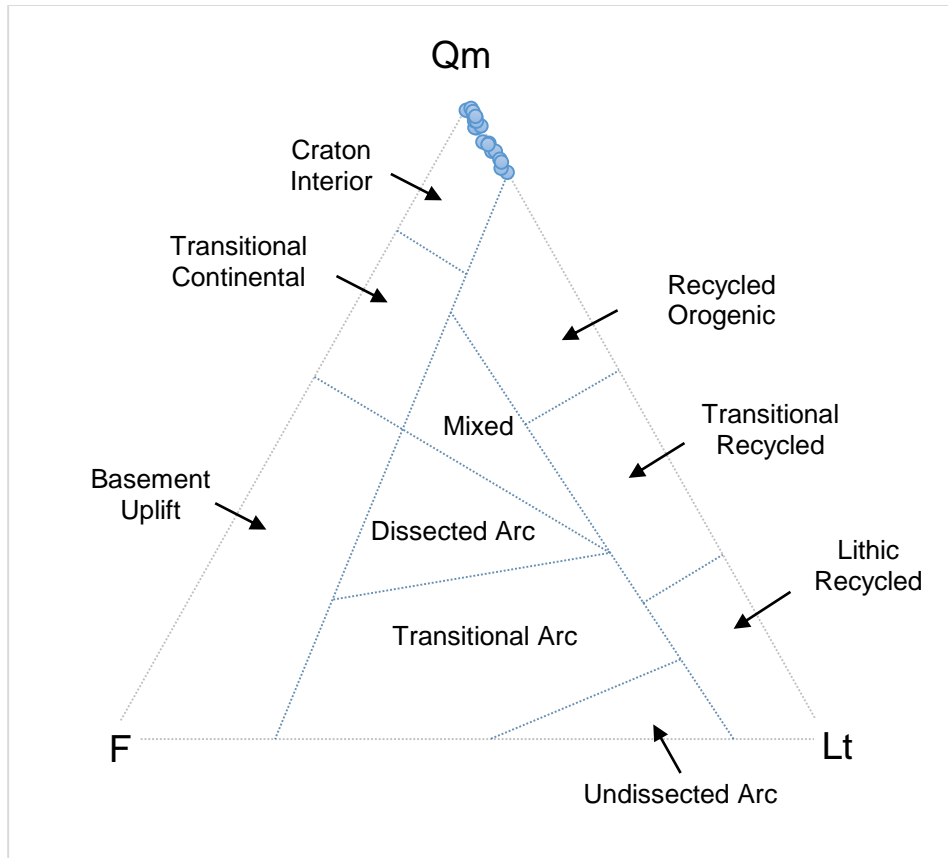
Figure 35. QmFLt ternary diagrams (Dickenson, 1985) of framework mineralogy for the Meridian Sand showing that sands and sandstones fall in the craton interior field.
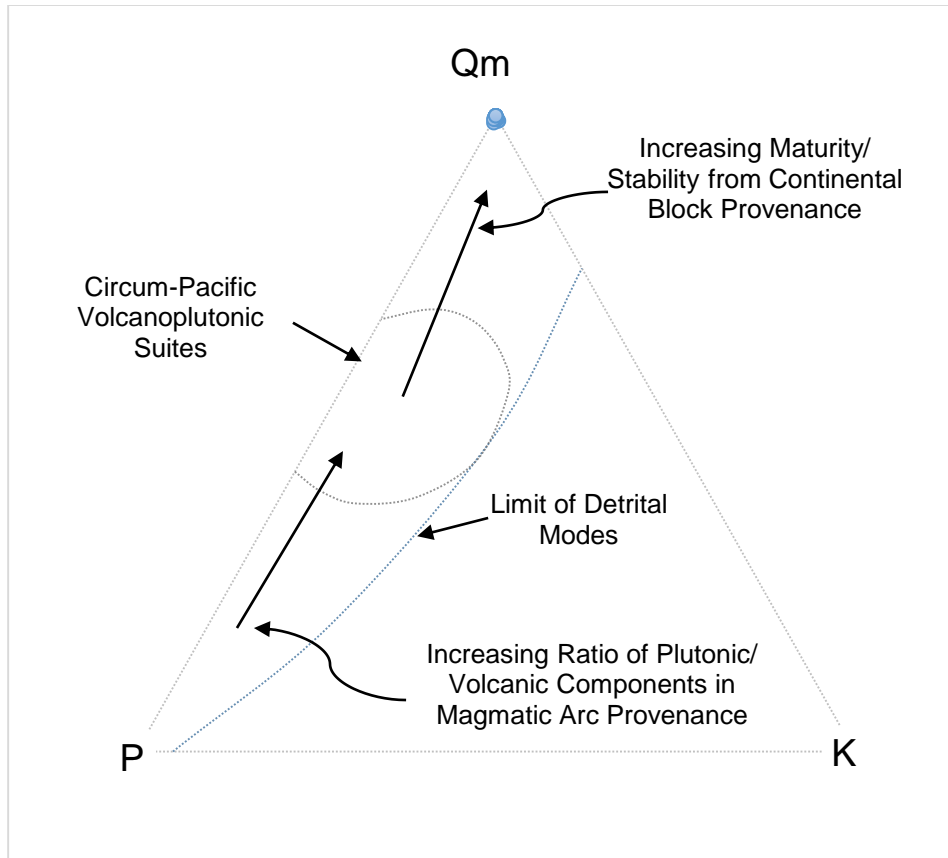
Figure 36 QmPK ternary diagram (Dickenson, 1985) of framework mineralogy
for the Meridian Sand showing an increase in maturity and stability from
a continental block provenance of sands and sandstones.
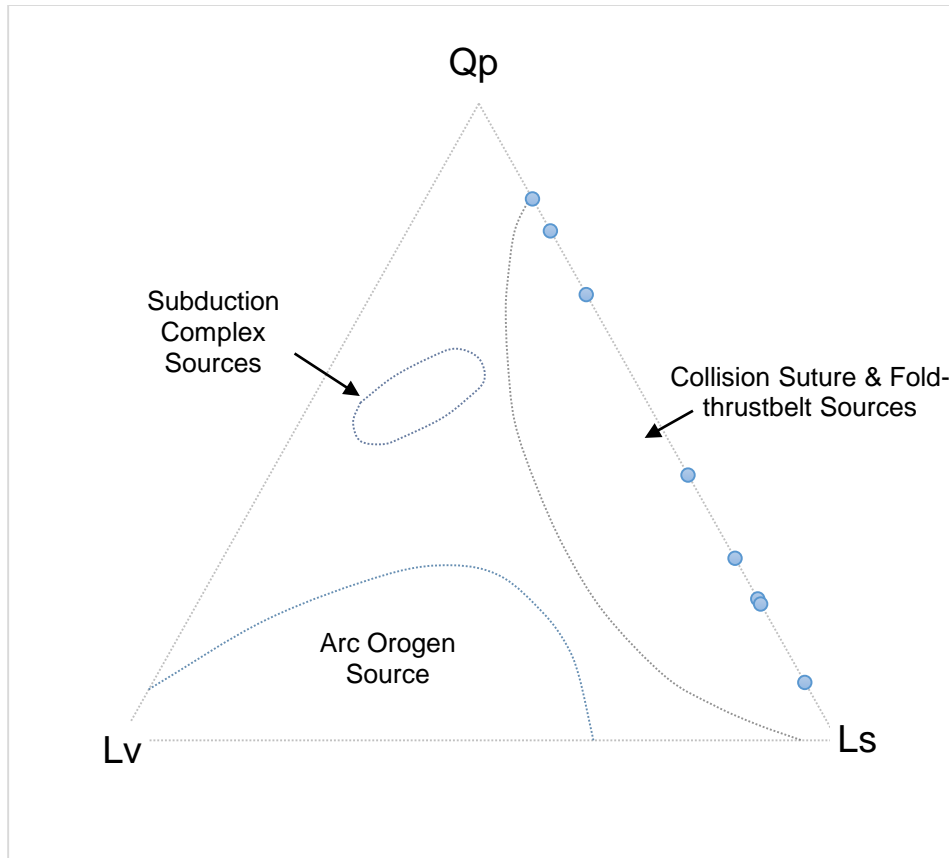
Figure 37. QPK ternary diagram (Dickenson, 1985) of framework mineralogy for the Meridian Sand showing sands and sandstones fall in the collision suture field.

Parent rock interpretation

The use of trace elements to interpret the composition of the parent rock was discussed
by McLennan (1989; 1993). Relative abundances of the trace elements Zr, Sc, Th can be an
indication of the characteristics of the parent rock (Bhatia & Crook, 1986; McLeen, 1986).
Figure. 38 shows Zr/Sc versus Th/Sc plots for all mud, sand and sandstone samples. All samples
are characterized by Zr/Sc ratios >10, indicating that these rocks were derived from a recycled
sedimentary source (McLennan, 1993). The absence of variation of Zr/Sc and Th/Sc indicates
that igneous rocks are not a major parent rock for siliciclastics of the Meridian Sand.

SiO_2/Al_2O_3 ratios can also provide an indication of the composition of the parent rock.
SiO_2/Al_2O_3 ratios that exceed 5 and 6 can indicate a recycled sedimentary source (Roser et al.,
1996). The majority of Meridian samples have high SiO_2/Al_2O_3 ratios (Fig. 39). Only two
samples (M5-03, and M5-06) have ratios < 5. The high ratio of SiO_2/Al_2O_3 might be related to
the high ratios of Q/F that can be seen in all samples. However, the low SiO_2/Al_2O_3 ratios of
samples M5-03 and M5-06 might be affected by diagenesis, which can influence provenance
interpretations (McLennan, 1993). Hence, preexisting sedimentary rocks are possibly a major
source for siliclastics of the Meridian Sand.

The mineral tridymite, which is present only in one mud-dominated sample, is a
polymorph of quartz that is only stable in volcanic environments. Tridymite is found in volcanic
rocks such as rhyolite, obsidian, and andesite (Klein & Hurlbut, 1993). Hence, these rocks might
be the source of tridymite found in muds of the Meridian Sand. These volcanic rocks might have
formed as a result of volcanic activity that occurred in the Late Cretaceous (Dockery et al.,
1997). This volcanic activity generated volcanic rocks with high silica content (Dockery et al.,
1997; Dockery and Thompson, 2016). Dockery et al. (1997) said that volcanic terrains formed in

the central region of the ME as a result of volcanic activity and this region includes the Jackson

Dome, the Monore Uplift, and southern Arkansas. These regions may be the source of the

tridymite found in Meridian mud sediments. Therefore, there may be a minor volcanic source for

Meridian sediments. The zeolite laumontite, which is also present in one mud-dominated sample

might result from alteration of volcanic glass in areas of volcanic activity (Boggs, 2012).

Previous studies (e.g., Reynolds, 1970; Dockery, 1986; Kabir & Panhorst, 2004) on mud rocks of

the Tallahatta Fm showed that zeolites were present and resulted from altered volcanic

pyroclastics.
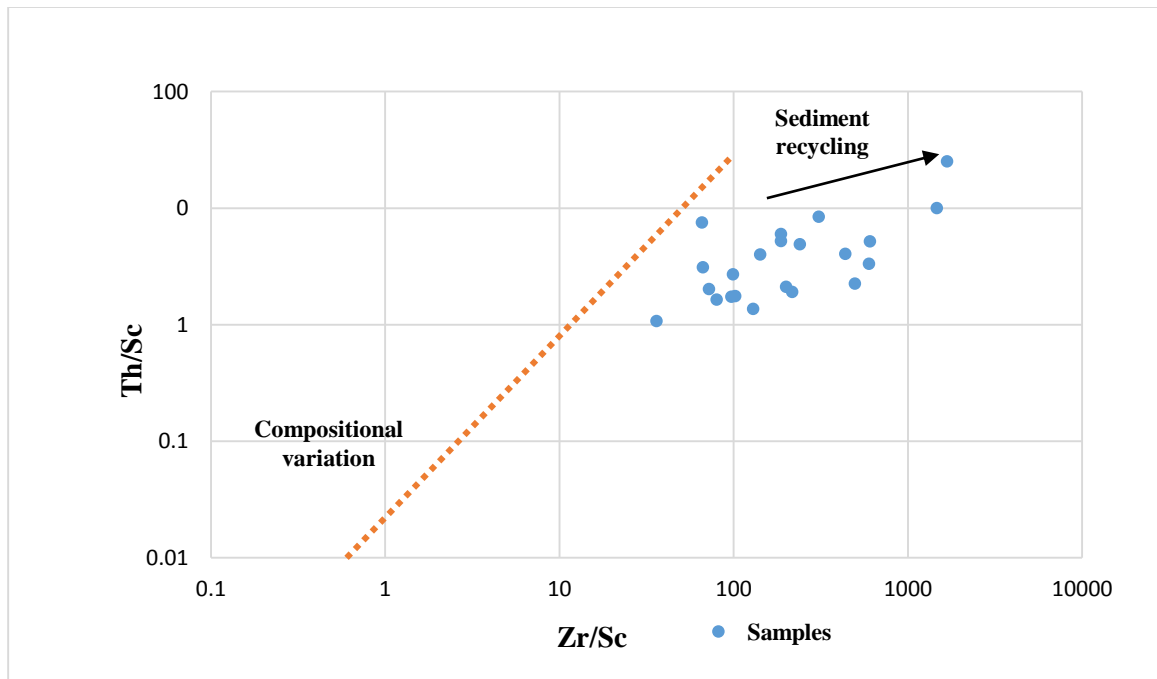
Figure 38. Th/Sc versus Zr/Sc plots of McLennan et al., (1993) for all samples from the Meridian Sand.
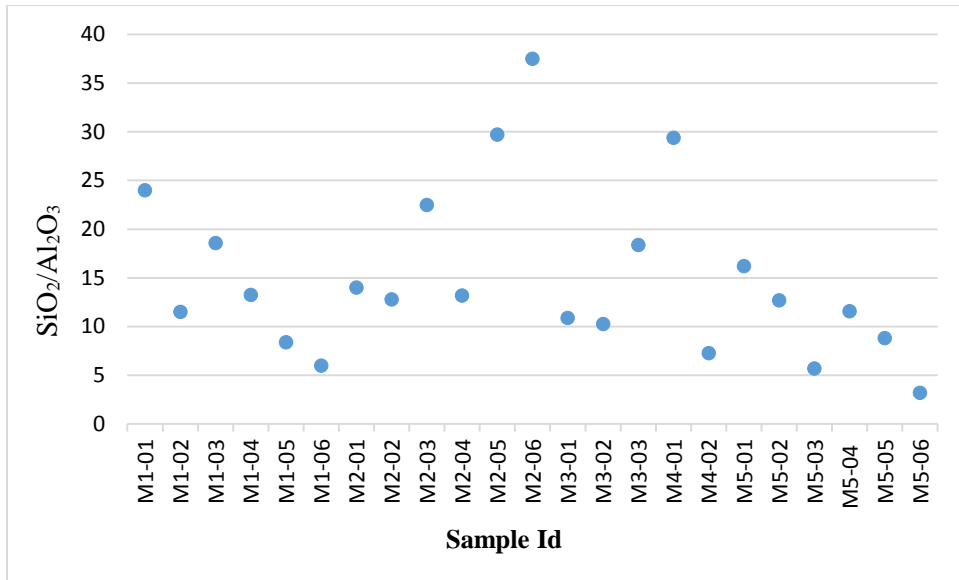
Figure 39. Plots of SiO_2/Al_2O_3 ratios for all 23 samples from the Meridian Sand.

The description of the nine lithofacies of the Meridian sand and their interpretations are provided in Table 2. Figure. 40 shows the stratigraphic position of each lithofacies.

Lithofacies 1

The presence of sand materials in this lithofacies and low amount of mud materials suggest that bedload deposition was predominant. The presence of mud clasts in this lithofacies might be the result from spring tides (Boggs, 1995). The lithofacies is interpreted to be deposited probably in a subtidal or foreshore settings.

Lithofacies 2

The poorly, very fine sand that composes this lithofacies contains some mud (matrix), suggesting deposition from bedload and suspension. The poor sorting of sand grains, as well as mud content, might reflect deposition in a lower intertidal (sand flat) setting (e.g., Desjardins et al., 2012).

Lithofacies 3

The relatively immature wacke that constitutes this lithofacies, which contains moderate mud sediments, reflects deposition in a relatively moderate to low energy setting. The mixing between mud and sand is characteristic of an intertidal flat, particularly, mixing flat environment, which occurs between sand and mud flats. The presence of sand lenses and mud sediments suggest deposition from bedload and suspension.

Lithofacies 4

The sand from this lithofacies represents bedload sediment deposition. However, thin mud beds that are found in the middle part of this lithofacies in section 1 indicate periods of slack water, where mud was deposited from suspension. The alternating mud and sand beds suggest deposition in a subtidal to intertidal (sand flat) setting (Boggs, 1995; Desjardins et al., 2012).

Lithofacies 5

This lithofacies is relatively thick in comparison with other lithofacies, and it is composed mostly of bedload sediment. The presence of cross-bedding, burrows, and mud clasts probably reflect deposition in moderate to high energy (Boggs, 1995; Desjardins et al., 2012). The possible environment for this lithofacies is subtidal to lower intertidal (sand flat).

Lithofacies 6

Flaser bedding and mud drapes in this lithofacies are an indication of deposition in an intertidal (mixing flat) setting. The presence of flaser bedding in this lithofacies suggests relatively brief slack water episodes where mud was deposited from suspension (probably on eroded ripple crests) (e.g., Boggs, 1995; James and Dalrymple, 2012). The presence of herringbone cross-stratification indicates changes in paleocurrent and also indicates deposition in a tidally influenced environment.

Lithofacies 7

The lithology of this lithofacies also reflects mainly bedload sediment deposition because it is mostly composed of mature, moderately sorted sand. The intensive presence of burrows suggests deposition in a lower intertidal (sand flat) setting.

Lithofacies 8

This lithofacies (Fig. 40) in comparison to other Meridian lithofacies does not show any evidences of a tidal flat environment such as mud drapes, flaser bedding, and lenticular bedding. The coarse sand forming this lithofacies might have been deposited under high energy, probably wave energy that can move and deposits coarser grains. In addition, this lithofacies contains *Ophiomorpha* burrows. This type of burrow can be an evidence that these beds may have been deposited in shoreface environment.

Lithofacies 9

Sediments in this lithofacies are very fine in comparison to other lithofacies, indicating deposition from suspended load. The lenticular bedding in this lithofacies indicates that mud content was dominant during deposition. The presence of lamination in the mud resulted from deposition in a low energy setting. The lithofacies is interpreted to be deposited in an intertidal setting, probably a muddy tidal flat.

The depositional environment interpretations of the lower Tallahatta Fm (Meridian Sand) is compatible with that of Sarvda et al. (2010) and Tarner (1993) that the Tallahatta Fm was deposited in marginal-marine environment. This study suggests that the lower Tallahatta Fm was deposited probably in a tidal flat environment based on the evidence from grain-size trends and field observations. A tidal flat environment was also suggested by Tarner (1993), who

studied sandstone rocks collected from the Tallahatta Fm near Meridian, MS. He also suggested that the Tallahatta Fm was deposited in low-energy beach and near-shore environments. The Tallahatta Fm in southern Alabama and southern-eastern Mississippi is interpreted by Sarvda et al., (2010) to have been deposited in a deeper setting, probably offshore and shoreface environments. Also, he mentioned that storm-wave conditions played were dominant during deposition of the Tallahatta Fm. He focused on ichnofossils on the Tallahatta Fm as indications of environment and energy. For example, he defined *Ophimorpha* burrows in sandstone beds of the Tallahatta Fm, and he suggested that these sandstone beds reflect deposition in shoreface to offshore environments. These types of burrows were observed in sandstone beds of the Meridian Sand in Grenada County, and used as an indication of deposition in a higher energy shoreface environment. However, most of Meridian lithofacies in Grenada County show good evidences of tidal flat environment, indicating that these rocks might have deposited landward. The differences in interpretations of depositional environment between this study and the studies of Tarner (1993) and Sarvda et al. (2010) are related to lithological heterogeneity of the Tallahatta Fm. It appears that, The Tallahatta siliciclastics in southern Mississippi and Alabama reflects deposition probably in deeper settings in comparison to Tallahatta sediments exposed in north portion of Mississippi.
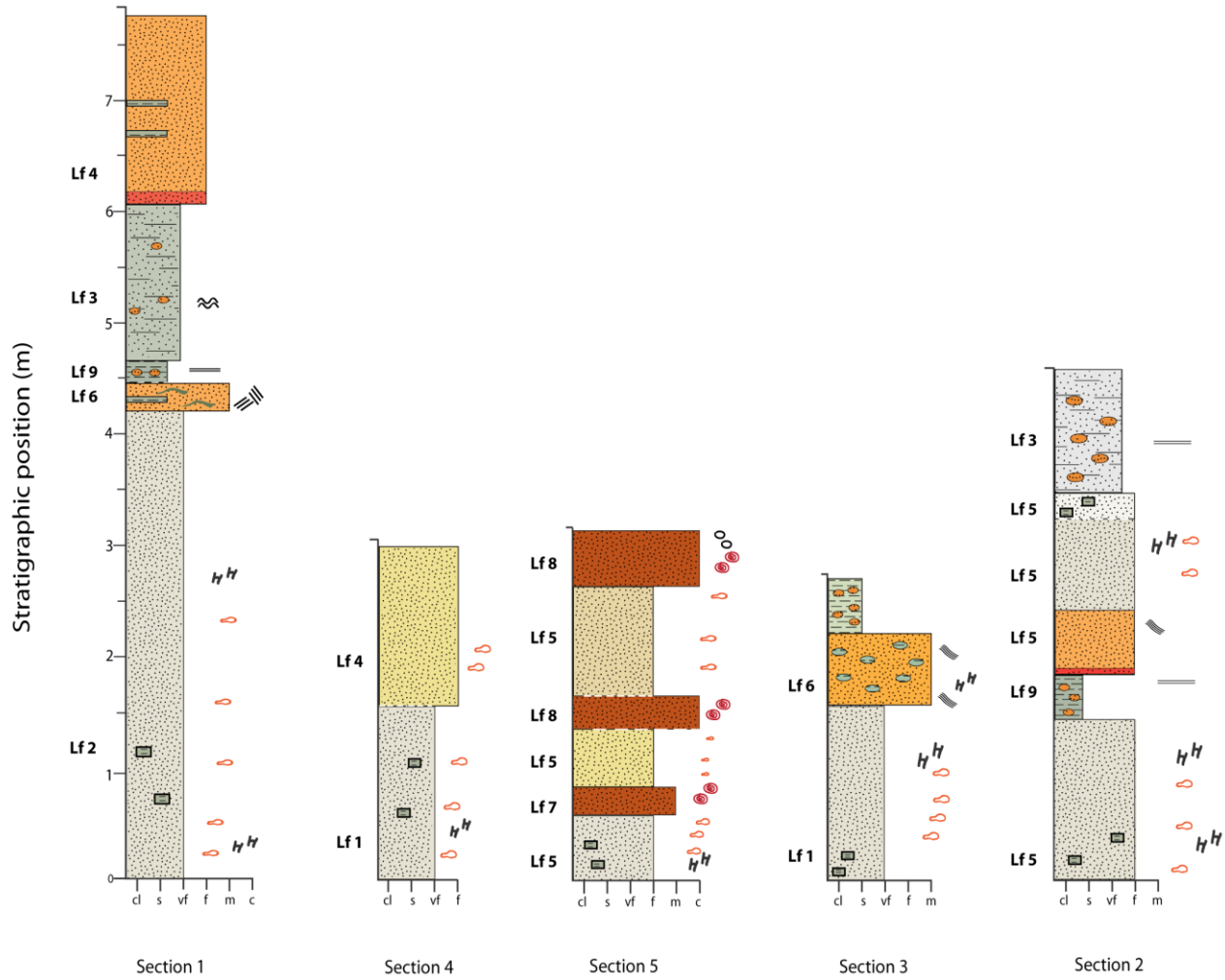
Figure 40. The five stratigraphic sections including the stratigraphic position of the nine lithofacies of the Meridian Sand. See figure 6 for explanations of symbols.

Diagenetic history

Diagenetic features within the Meridian Sand include bioturbation, cementation, grain dissolution, and compaction. Trace fossils associated with sand and sandstone beds in the Meridian Sand resulted from organisms reworking sediment shortly after deposition. In red sandstones in section 5, Fe- cemented *ophiomorpha* burrows are present (Fig. 23). In these deposits, the organism reworking occurred first, followed by cementation by hematite. Hematite might have been precipitated within burrow walls when the fluids moved through the organism-constructed pathways. The trace fossils found in the Meridian Sand are indications of early diagenesis (eogenesis).

The hematite cement that coats some sand grains might have formed in the early stages of diagenesis. In red sandstone deposits from section 5, hematite cement (Fig. 26E) is also found in the samples that were collected from beds where Fe- cemented burrows are present. In this case, hematite cement coating sand grains, and hematite within walls of burrow pathways might have been formed at the same time. Hematite cement in these samples likely precipitated during eogenesis (Fig. 41) due to the fact that the Fe oxides can be formed either during eogenesis or telogenesis (Burley & Worden, 2003). This interpretation is made because there is not abundant evidence that these sands and sandstones underwent middle and late stages of mesogenesis, hence they might not have experienced much exhumation. In addition, some friable sand samples contain hematite cement, and that can be evidence that these sands probably did not undergo mesogenesis or telogenesis. Some of the samples that are characterized by hematite cement that coats the grains also contain clay cement (Fig. 26C). In these samples, the hematite cement appears to have precipitated first, followed by the clay cement that filled the remaining pore

space. The clay cement does not coat the grains, indicating that the hematite cement precipitated first (Fig. 26C). Clay cement, which is distinguished by its brown color, is found around the grain boundaries in sample M3-01 and might have been formed before compaction because the clay is also found along the grain contacts (Fig. 26A). Clay cement in sandstones occurs as a burial diagenetic cement (Burley & Worden, 2003). The presence of clay cement in some samples might be evidence of relatively shallow burial, and it might have precipitated during eogenesis (Fig. 41). The possible hydrocarbon staining in sandstone samples from section 5 is an indication of oil migration that might have occurred after the cementation of hematite (Fig. 26E). Oil migration might have started during eogenesis after the cementation of hematite or during mesogenesis, depending on the depth of the source rocks.

Partial dissolution of quartz grains (Figs. 27C), which is seen in a few samples, might have resulted from pore fluids capable of dissolving silica, high temperature, or high stresses (Burley & Worden, 2003). Because there is not enough evidence of intensive compaction, such as pressure solution, dissolution of quartz grains might have been caused by the fluids at relatively shallow depths during early mesogenesis (Burley & Worden, 2003) (Fig. 41). The point to point contacts and bending of muscovite that are found in a few samples (Figs. 27A & 27B) are evidence of a relatively low degree of compaction that might have occurred during late eogenesis or early mesogenesis (Fig. 41). The fractured quartz grains (Fig. 27D), which would normally indicate deep burial, are not associated with any other indicators of late mesogenesis, indicating that they may have been fractured within the source sedimentary rocks. If this is true, they may be a potentially useful marker bed within the Meridian Sand. The overall interpretation of the diagenesis of sands and sandstones suggest that the Meridian Sand underwent eogenesis and early mesogenesis (Fig. 41).

Diagenetic stages/processes	Eogenesis	Mesogenesis	Telogenesis
Hematite cement	▬		
Clay cement	▬		
Compaction	▬▬▬ – –		
Dissolution		▬ – –	

Figure 41. Paragenetic sequence of sands and sandstones of the Meridian Sand Member.

CONCLUSION

This research was carried out to study the petrology of the Meridian Sand to interpret the provenance, depositional environment, and diagenetic history of Meridian sediments in Grenada County, MS. Five locations in Grenada county were studied, and 23 bulk mud, sand, and sandstone samples were collected in total. Mineralogical, geochemical and textural analyses were performed on all samples. The lithology of the Meridian Sand in Grenada County is very fine to coarse, poorly to moderately well sorted, angular to sub-angular sand and sandstone, and it is interbedded with mud.

Petrographic study and modal analyses of 21 thin-sections of sand and sandstones showed that quartz is the most dominant mineral, making up ~> 90% of the total sands. Feldspar is a minor constituent of the Meridian Sand, whereas, sedimentary lithics represent ~4% of the total grains. According to Dott's (1964) classification, the Meridian Sand includes quartzarenite, sublitharenite, quartzwacke, and lithicgrawake.

Provenance interpretations of sand and sandstone samples using ternary diagrams of Dickenson (1985) suggest two possible provenances for the Meridian sediments. Most samples from the Meridian Sand appear to be sourced from the craton interior and a recycled orogen province due to the high content of monocrystalline quartz grains. Some very fine and rounded zircons were found in some samples, and they are similar to those described by Grim (1936)

from a distal Appalachian source. These zircons differ from the angular to sub-angular quartz framework grains and might have been sourced from the Appalachians.

Geochemical results for all samples show that all samples are rich in SiO_2, which ranges from 76.1 to 95.5%. Zr is the most abundant trace element, and it has an average of 318.6 ppm. High SiO_2/ Al_2O_3 ratios and Zr enrichment may indicate a sedimentary source for Meridian sediments. The mineralogical composition of two mud samples shows populations of quartz, clay minerals, muscovite, laumontite, and tridymite. Tridymite might be an indication of a minor volcanic source that probably formed as a result of volcanic activity that occurred in the ME during the Late Cretaceous.

Sedimentary structures include flaser bedding, lenticular bedding, cross-bedding, herringbone cross stratification, mud clasts, mud drapes, and burrows. These features, in addition to grain-size trends, indicate that the Meridian Sand was deposited largely in a tidal flat and shoreface environment.

Diagenetic features in the sands and sandstones of the Meridian Sand include clay and hematite cements, dissolution of quartz grains, minor compaction, and hydrocarbon staining. These diagenetic features suggest that the Meridian Sand underwent eogenesis and early mesogenesis.

REFERENCES

Adams, R.W.,1943, Geology and groundwater supply at Camp McCain: Mississippi Geological Survey Bulletin 55, 166 p.

Bhatia, Mukul.R. and Keith, A. and Crook. W., 1986, Trace Element Characteristics of Graywackes and Tectonic Setting Discrimination of Sedimentary Basins: Contributions to Mineralogy and Petrology, v. 92, p. 181–193.

Blott, S.J., and pye, K., 2001, Gradistat: A Grain Size Distribution and Statistics Package For The Analysis Of Unconsolidated Sediments: Earth Surface Processes And Landforms, V. 26, P.1237-1248.

Boggs, Sam., 1995, Principles of sedimentology and stratigraphy: Pearson Education, New Jersey, 655 p.

Boggs, Sam., 2012, Petrology of sedimentary rocks: Cambridge university press, Cambridge, 596 p.

Brown, G.F., 1947, Geology and artesian water of the alluvialplain in northwestern Mississippi: Mississippi Geological Survey, Bulletin 65, 424 p.

Burke, Kevin. and J. F. Dewey, J.F., 1973, Plume-Generated Triple Junctions: Key Indicators in Applying Plate Tectonics to Old Rocks: The Journal of Geology, v. 81, p. 406–433.

Bybell, L.M. and Gibson, T.G., 1985, The Eocene Tallahatta Formation of Alabama and Georgia: Its lithostratigraphy, biostratigraphy, and bearing on the age of the Clairbornian Stage: United States Geological Survey, Bulletin 1615, 20 p.

Chen C.S.,1965, The regional lithostratigraphic analysis of Paleocene and Eocene rocks of Florida.Flor: Geol. Surv. Bull., v. 45, 97 p.

Cook, T.D. and Bally, A.W., 1975, Stratigrapghic Atlas of North and Central America: Princeton University Press, Princeton, NJ, 231 p.

Count, J.W., Bigham. E. and MARTIN, S., 2010, Ichnology of siliceous facies in the Eocene Tallahatta Formation (eastern united states Gulf Coastal Plain): Implications for depositional conditions, storm processes, and diagenesis: Palaios, v. 10, p. 642-655.

Cox, R.t. and Van Arsdale, R.B., 1997, Hotspot Origin of the Mississippi Embayment and Its Possible Impact on Contemporary Seismicity: Engineering Geology, v. 46, p. 201–216.

Cushing, E.M. Boswell, E.H. and Hosman, R.L., 1964. General geology of the Mississippi Embayment:United States Geological Survey Professional Paper, no. 448-B, p. 1-25.

Craddock, W. H., and A. R. C. Kylander-Clark., 2013, U-Pb Ages of Detrital Zircons from the Tertiary Mississippi River Delta in Central Louisiana: Insights into Sediment Provenance." Geosphere, vol. 9, p. 1832–1851.

Desjardins, Patricio R. Buatois, Luis. Gabriel, Mangano. M. Gabriel, 2012, Tidal Flats and Subtidal Sand Bodies: Developments in Sedimentology Trace Fossils as Indicators of Sedimentary Environments, v. 64, p. 529–561.

Denison, R.E., 1984, Basement rocks in northern Arkansas, in Mc-Farland, J.D., and Bush, W.V., eds., Contributions to the Geology of Arkansas: Arkansas Geological Commission Miscellaneous Publication 18-B, v. II, p. 33-49.

Dickingson, William. R. and Christopher, A. Suczek., 1979, Plate Tectonic and Sandstone Composition: The American Association of Petroleum Geologists, v. 63, p. 2164–2182.

Dickinson, W.R. Beard, L.S. Brakenridge, G.R. Erjavec, J.L. Ferguson, R.C. Inman,K.F. Knepp, R.A. Lindberg, F.A. and Ryberg, P.T., 1983, Provenance of North American Phanerozoic sandstones in relation to tectonic setting: Geological Society of America Bulletin, v. 94, p. 222-235.

Dickinson, William. R., 1985, Interpreting provenance relations from detrital modes of Dockery, sandstones: Provenance of arenites, v. 148, p. 333-361.

Dockery, D.T., 1986, The Bashi-Tallahatta section at Mt. Barton, Meridian, Mississippi, in Neathery, T.L., ed., Centennial Field Guide, vol. 6: Geological Society of America, Boulder, Colorado, p. 383–386.

Dockery., David. T. Marble. Tohn. C. and Henderson. Jack., 1997, The Jackson Volcano: The department of environmental quality, Jackson, Mississippi, v. 18, p. 33-55.

Dockery, D.T. and Thompson, D.E., 2016, The geology of Mississippi: University press of Mississippi, Jackson, 692 p.

Dott, Jr. R. H., 1964, Wacke, Graywacke and Matrix--What Approach to Immature Sandstone Classification? :SEPM Journal of Sedimentary Research, v. 34, p. 625–632.

Ervin, C. Patrick. and Mcginnis, L.D., 1975., Reelfoot Rift: Reactivated Precursor to the Mississippi Embayment: Geological Society of America Bulletin, v. 86, p. 1287–1295.

Fisher, W.L. and Mcgowen, J.H., 1967., Depositional Systems in Wilcox Group of Texas and Their Relationship to Oil and Gas Occurrence: AAPG Bulletin, v. 7, p. 105–125.

Galloway W.E., 1968, Depositional systems of the Lower Wilcox Group, north-central Gulf Coast Basin: Gulf Coast Assoc. Geol. Socs, v. 18, p. 275-289.

Garzanti, Eduardo., 2016, The Maturity Myth in Sedimentology and Provenance
        Analysis: Journal of Sedimentary Research, v. 87, p. 353–365.

Gilliland, W.A. and Harrelson, D.W., 1980, Clark county geology and mineral recourses: Bureau
        of Geology, Jackson, 201 p.

Grim, R. E., 1936, The Eocene sediments of Mississippi: Mississippi Geological Survey Bulletin
        30, 240. p.

Ham, W. E. and. Wilson, J.L., 1967, Paleozoic Epeirogeny and Orogeny in the Central United
        States: American Journal of Science, v. 265, p. 332–407.

Hildenbrand, T.G. and J.d. Hendricks, J.D., 1995, Geophysical Setting of the Reelfoot Rift and
        Relations between Rift Structures and the New Madrid Seismic Zone: U.S. Geological
        survey professional paper 1538- E, p. 1–27.

James. Noel. P. and Dalrymple, Robert. W., 2010, Facies Models: Geological Association of
        Canada, Canda. 577 p.

Kabir, S. and Panhorst, T., 2004, Origin of Gulf coast opal-CT: A case study of the
        claystone-rich Tallahatta Formation in Mississippi: Southeastern Geology, v. 42, p.
        151–163.

Klein, C. and Hurlbut jr. C.S., 1993. Manual of mineralogy: New York, 681 p.

Low, E.N., 1915, Mississippi, its geology, geography, soils and mineral resources: Mississippi
        Geological Survey, v. 12, 335 p.

Lowe, E.N., 1933, Midway and Wilcox Groups: Mississippi State Geological Survey,
        University, Mississippi, V. 25, 125 P.

McGinnis, L D., 1963, Earthquakes and Crustal Movement as Related to Water Load in the
        Mississippi Vally Region: Illinois State Geological Survey Circular, p.1- 20.

McLennan, Scott. M. Hemming, S. Mcdaniel. D.K. and Hanson.G.N., 1993, Geochemical
        Approaches to Sedimentation, Provenance, and Tectonics: Special Paper of the Geological
        Society of America, v. 284, p. 21–40.

McLennan, Scott. M., 1989, Rare Earth Elements in Sedimentary Rocks: Influence of
        Provenance and Sedimentary Process: Review of Mineralogy, v. 21, p. 169–200.

Merrill, R.K. Sims, J.J. Gann, D.E. and Liles, k.J., 1985, Newton county geology and mineral
        resources: Mississippi Bureau of Geology, Jackson, MS, V. 126, 108 p.

Murray, G.E., 1961, Geology of the Atlantic and gulf coastal Province of north America: Harper and Brothers, New York, NY, 692 p.

Reed, J.C. Wheeler, J.O. and Tucholk, B.E., 2004, Geologic map of North America: Decade of North American geology continental scale map 001. Boulder, Geolgical survey of America.

Reynolds, W.R., 1970, Mineralogy and stratigraphy of Lower Tertiary clays and claystones of Alabama: Journal of Sedimentary Petrology, v. 40, p. 829–838.

Reynolds, W.R., 1992, The heavy mineral population within the beach sand facies of the Meridian Sand exposed in Mississippi: Gulf Coast Association of Geological Societies, v. 42, p. 633–646.

Roser, B.P. Cooper, R.A. Nathan, S. and Tulloch, A.J., 1996, Reconnaissance sandstone Savrda, geochemistry, provenance, and tectonic setting of the lower Paleozoic terraines of the West Coast and Nelson, New Zealand: New Zealand. J. Geol. Geophys, v. 39, p. 1-16.

Stearns, Richard.G. and Marcher, Melvin.V., 1962, Late Cretaceous and Subsequent Structural Development of the Northern Mississippi Embayment Area: Geological Society of America Bulletin, v. 73, p. 1387–1394.

Stenzel, H. B., 1952, Correlation chart of Eocene at outcrop in eastern Texas, Mississippi, and western Alabama: Mississippi Geol, Guidebook, 9th field trip, p. 32-33.

Suttner, Lee J., 1974, Sedimentary Petrographic Provinces: An Evaluation: Paleogeographic Provinces and Provinciality, p. 75–84.

Tanner., William. F., 1993, Enviromental analyses of sandstone and quartzites from the Tallahatta Formation, near Meridian, Mississippi: The department of environmental quality, Jackson, Mississippi, v. 4, p. 61-69.

Thomas, E.P., 1942. The Claiborne. Mississippi Geological Survey Bulletin 48, 96 p.

Thomas, William. A., 1989, The Appalachian-Ouachita Orogen beneath the Gulf Coastal Plain between the Outcrops in the Appalachian and Ouachita Mountains: The Appalachian-Ouachita Orogen in the United States, v. f-2 p. 537–553.

Tolmun., 1977, Stratigraphic distribution of Paleocene and Eocene fossils in the eastern Gulf Coast region: Alabama Geological Survey, University, 602 p.

LIST OF APPENDICES

APPENDIX I

Table 4. Sieve analyses results for 19 sand and mud samples from the Meridian Sand.

Sample weight	Sample No	Sieve No	Sieve size (MM)	Phi	Weight of sieve	Weight of sieve and sed	Weight of sed (g)	Retained %	Cumulative %	Passing %
M1-01	271.91 g	18	1	0	359.3	359.3	0	0	0	100
		35	0.5	1	310.3	310.4	0.1	0	0	100
		60	0.25	2	271	272	1	0.36	0.396	99.604
		120	0.125	3	257.7	399.4	141.1	51.89	52.286	47.714
		230	0.625	4	254	265.8	108.6	39.93	92.216	7.784
		Ban	<0.625	>4	526.1	546.1	20	7.35	99.56	--
M1-02	245.6 g	18	1	0	359.2	359.4	0.2	0.081	0.081	99.919
		35	0.5	1	310.3	313.2	2.9	1.18	1.26	98.74
		60	0.25	2	271	420.01	149.01	60.67	61.93	38.07
		120	0.125	3	257.8	342.01	84.21	34.28	96.21	3.79
		230	0.625	4	254	256.3	5.2	2.11	98.32	1.68
		Ban	<0.625	>4	526.1	529.8	3.7	1.5	99.82	--
M1-03	45.9 g	18	1	0	359.2	359.2	0	0	0	100
		35	0.5	1	310.3	310.3	0	0	0	100
		60	0.25	2	271	271	0	0	0	100
		120	0.125	3	257.8	257.8	0	0	0	100
		230	0.625	4	254	257.1	3.1	6.75	6.75	93.25
		Ban	<0.625	>4	526.1	568.9	42.8	93.24	13.5	--
M1-04	67.71	18	1	0	359.3	359.3	0	0	0	100
		35	0.5	1	310.4	310.4	0	0	0	100
		60	0.25	2	271	271	0	0	0	100
		120	0.125	3	257.8	269.9	12.1	17.87	17.87	82.13

		230	0.625	4	254	271.3	32.7	48.29	66.16	33.84
		Ban	<0.625	>4	526.1	548.6	22.5	33.22	99.38	--
M1-05	231.48 g	18	1	0	359.3	259.4	0.1	0.04	0.04	99.96
		35	0.5	1	310.4	312.3	1.9	0.82	1.68	98.32
		60	0.25	2	271	302.7	31.7	13.69	15.37	84.63
		120	0.125	3	257.8	433.5	175.7	75.9	91.27	8.73
		230	0.625	4	254	257.4	13.8	5.96	97.22	2.78
		Ban	<0.625	>4	526.1	533.3	7.2	3.11	100.3	--
M1-06	300.72 g	18	1	0	359.3	359.4	0.1	0.033	0.033	99.96
		35	0.5	1	310.4	313.4	3	0.99	1.023	98.97
		60	0.25	2	271	357.9	86.9	28.89	29.91	70.09
		120	0.125	3	257.8	453.1	195.3	64.94	94.85	5.15
		230	0.625	4	254	256.3	9.3	3.09	97.93	2.07
		Ban	<0.625	>4	526.1	531.1	5	1.66	99.59	--
M2-01	141.1 g	18	1	0	359.3	359.3	0	0	0	100
		35	0.5	1	310.3	310.3	0	0	0	100
		60	0.25	2	271	299	28	19.84	19.84	80.16
		120	0.125	3	253.7	348.1	94.4	66.9	86.74	13.26
		230	0.625	4	254.2	263.7	9.5	6.73	93.47	6.53
		Ban	<0.625	>4	525.9	536.9	11	7.79	101.26	--
M2-02	39.45 g	18	1	0	359.3	359.3	0	0	0	100
		35	0.5	1	310.4	310.4	0	0	0	100
		60	0.25	2	271	271	0	0	0	100
		120	0.125	3	257.8	257.8	0	0	0	100

		230	0.625	4	225.7	236.25	10.55	26.74	26.74	73.26
		Ban	<0.625	>4	524	552.9	28.9	73.25	99.99	--
M2-03	150.01	18	1	0	359.3	359.3	0	0	0	100
		35	0.5	1	310.3	311.2	0.9	0.59	0.59	99.41
		60	0.25	2	271	313.1	42.1	28.06	28.65	71.35
		120	0.125	3	257.8	343.5	85.7	57.12	85.77	14.23
		230	0.625	4	254.1	265.5	11.4	7.59	93.36	6.64
		Ban	<0.625	>4	525.9	534.3	8.4	5.59	98.95	--
M2-04	181.7	18	1	0	359.3	359.3	0	0	0	100
		35	0.5	1	310.3	313.3	3	1.65	1.65	98.35
		60	0.25	2	271	317.3	46.3	25.48	27.13	72.87
		120	0.125	3	257.8	369	111.2	61.19	88.32	11.68
		230	0.625	4	254.1	267.8	13.7	7.53	95.85	4.15
		Ban	<0.625	>4	525.9	533.6	7.7	4.23	100.08	--
M2-06	44.7	18	1	0	359.3	359.3	0	0	0	100
		35	0.5	1	310.4	310.5	0	0.22	0.22	99.78
		60	0.25	2	271	275.8	4.8	10.71	10.93	89.07
		120	0.125	3	257.8	269.3	14.5	32.36	43.29	56.71
		230	0.625	4	254.1	268	12.3	27.45	70.74	29.26
		Ban	<0.625	>4	525.9	555.5	13.1	29.24	99.95	--
M3-01	91.3	18	1	0	341.2	341.2	0	0	0	100
		35	0.5	1	210.3	210.4	0.1	0.1	0.1	99.9
		60	0.25	2	271	274.3	3.3	3.61	3.71	96.29
		120	0.125	3	257.6	304.4	46.8	51.25	54.96	45.04
		230	0.625	4	253.9	276.8	22.9	25	79.96	20.04
		Ban	<0.625	>4	525	542.1	17.1	18.72	98.68	--

M3-02	80.5	18	1	0	341.2	341.2	0	0	0	100
		35	0.5	1	310.2	310.4	0.2	0.24	0.24	99.76
		60	0.25	2	271	274	3	3.72	3.96	96.04
		120	0.125	3	257.7	295.5	37.8	46.95	50.91	49.09
		230	0.625	4	254	278.5	24.5	30.43	81.34	18.66
		Ban	<0.625	>4	525.1	539.8	14.7	18.26	99.6	--
M3-03	168.1	18	1	0	241.2	241.2	0	0	0	100
		35	0.5	1	310.3	316.6	6.3	3.74	3.74	96.26
		60	0.25	2	271.1	354.3	83.2	49.49	53.23	46.77
		120	0.125	3	257.7	327	69.3	41.22	94.45	5.55
		230	0.625	4	253.9	260.5	6.6	3.92	98.37	1.63
		Ban	<0.625	>4	525.2	527.1	1.9	1.13	99.5	--
M4-01	82.7	18	1	0	341.1	341.1	0	0	0	100
		35	0.5	1	310.2	310.3	0.1	0.12	0.12	99.88
		60	0.25	2	271	272.6	1.6	1.93	1.72	98.28
		120	0.125	3	257.7	286.3	28.6	34.58	36.3	63.7
		230	0.625	4	254	290.3	36.3	43.89	80.19	19.81
		Ban	<0.625	>4	525.1	541.6	16.5	19.95	100.1	--
M4-02	152.3	18	1	0	341.2	341.2	0	0	0	100
		35	0.5	1	310.3	310.3	0	0	0	100
		60	0.25	2	271	279	8	5.25	5.25	94.75
		120	0.125	3	257.6	350.5	92.9	60.99	66.24	33.76
		230	0.625	4	253.9	293.5	39.6	26	92.24	7.76
		Ban	<0.625	>4	525.1	536.5	11.4	7.48	99.72	--
M5-01	81.7	18	1	0	341.3	341.3	0	0	0	100

		35	0.5	1	310.5	310.9	0.4	0.48	0.48	99.52
		60	0.25	2	271	280.1	9.1	11.13	11.61	88.39
		120	0.125	3	258	307.4	49.4	60.46	72.07	27.93
		230	0.625	4	244.5	263.1	18.6	22.76	94.83	5.17
		ban	<0.625	>4	367.4	371.6	4.2	5.14	99.97	--
M5-03	129.7	18	1	0	241.2	241.2	0	0	0	100
		35	0.5	1	310.3	312.1	1.8	1.38	1.38	98.62
		60	0.25	2	271	321.3	50.3	38.78	40.16	59.84
		120	0.125	3	257.6	325.3	67.7	52.19	92.35	7.65
		230	0.625	4	253.9	260.8	6.9	5.31	97.66	2.34
		Ban	<0.625	>4	525.1	528.1	3	2.31	99.97	--
M5-05	73.9	18	1	0	341.2	341.2	0	0	0	100
		35	0.5	1	310.3	313.1	2.8	3.78	3.78	96.22
		60	0.25	2	271	287.4	16.4	22.19	25.97	74.03
		120	0.125	3	257.6	297	39.4	53.31	79.28	20.72
		230	0.625	4	253.9	264.1	10.2	13.8	93.08	6.92
		Ban	<0.625	>4	525.1	530.2	5.1	6.9	99.98	--

APPENDIX II

Table 5. Grain- size data for all 23 samples collected from the Meridian Sand.

Sample ID	Mean grain size Phi	STDev Phi	Skewness	Kurtosis
M1-01	3.03	1.31	0.08	0.14
M1-02	1.91	0.67	1.09	4.89
M1-03	4.33	0.25	-3.38	12.56
M1-04	3.63	0.75	-0.09	1.51
M1-05	2.66	0.71	-0.23	4.29
M1-06	2.24	0.59	0.43	5.68
M2-01	2.55	0.76	1.64	3.3
M2-02	-	0.44	-1.03	2.11
M2-03	2.45	0.77	0.66	3.95
M2-04	2.37	0.73	0.62	4.75
M2-05	2.71	0.97	0.49	2.6
M2-06	3.24	0.99	1	2
M3-01	3.05	0.83	0.4	2.38
M3-02	3.11	0.82	0.35	2.45
M3-03	1.97	0.68	0.66	0.94
M4-01	3.33	0.76	-0.04	2.39
M4-02	2.85	0.64	0.95	5.02
M5-01	2.7	0.79	2.85	8.13
M5-02	1.4	0.71	0.82	2.05
M5-03	2.18	0.85	1.34	4.57
M5-04	0.39	1.43	2.73	7.72
M5-05	2.75	0.92	-0.54	3.08
M5-06	0.41	1.09	1.52	6.37

APPENDIX III

Table 6. Major oxides values for all 23 samples from the Meridian Sand. All values are in percent.

Sample ID	SiO_2	Al_2O_3	K_2O	CaO	Fe_2O_3	MnO	TiO_2
M1-01	93.22	3.73	0.49	0.16	1.41	0.001	0.98
M1-02	86.8	7.54	0.75	0.28	4.11	0	0.57
M1-03	89.54	4.82	1.2	0.173	1.86	0.007	2.33
M1-04	86.36	6.52	1.44	0.26	3.42	0.001	1.94
M1-05	80.25	9.57	0.61	3.61	8.79	0	0.49
M1-06	76.17	12.66	0.86	0.36	8.8	0	1.13
M2-01	76.17	5.44	0.52	0.25	3.92	0	0.38
M2-02	89.45	6.99	1.18	0.71	4.37	0	1.32
M2-03	85.39	3.85	0.3	0.17	1.84	0	0.45
M2-04	93.35	7.08	0.71	0.3	4.87	0	0.46
M2-05	86.67	2.92	0.24	0.098	1.56	0	0.16
M2-06	95	2.53	0.25	0.18	0.93	0.001	0.56
M3-01	95.51	8.77	0.96	0.4	6.1	0	0.56
M3-02	83.25	8.12	0.69	0.29	5.96	0	0.46
M3-03	84.44	4.59	0.52	0.06	2.54	0	0.34
M4-01	91.9	3.08	0.36	0.6	1.53	0	0.3
M4-02	89.1	12.27	5.28	0.33	7.66	0	0.5
M5-01	77.95	4.81	1.88	0.52	3.09	0.007	0.56
M5-02	89.11	7.02	0.79	0.3	7.69	0	0.28
M5-03	83.88	14.58	1.23	0.9	14.54	0.014	0.36
M5-04	68.32	5.89	0.77	0.28	4.05	0.001	0.46
M5-05	88.53	10	0.91	0.43	8.32	0.02	0.48
M5-06	47.9	24.68	1.16	0.43	26.03	0.19	0.26

Table 7. Trace element values for 23 samples (part 1) from the Meridian Sand. All values are in ppm.

Sample ID	S	Cl	Sc	V	Cr	Co	Ni	Cu	Zn	Ga	Ge	As
M1-01	0	48.309	0.517	0	16.726	12.006	5.495	0	21.307	3.567	1.483	0.569
M1-02	28.331	0	1.555	47.746	41.886	0	13.522	12.476	21.818	8.922	1.337	6.634
M1-03	67.564	194.074	0.519	25.318	28.868	2.686	12.79	0	38.727	17.23	1.201	1.067
M1-04	24.317	129.591	1.615	36.986	36.571	0	17.692	3.118	38.876	20.279	1.261	0.263
M1-05	0	103.269	0	17.612	15.559	0	11.297	8.051	14.621	2.392	0.964	1.533
M1-06	0	46.081	0.462	38.278	54.008	0	14.153	5.605	26.261	7.257	0.692	11.925
M2-01	0	0	1.625	34.588	13.344	19.413	15.122	0.327	33.76	1.946	1.99	10.789
M2-02	0	35.916	3.145	53.248	48.719	9.359	28.087	13.598	95.722	24.838	0.754	0.696
M2-03	0	17.683	0.595	13.183	4.972	0	10.292	0	35.071	0.547	1.15	8.994
M2-04	22.972	42.248	1.701	37.823	28.075	0	17.244	0	37.68	6.987	1.705	10.798
M2-05	0	93.777	0.558	9.158	12.778	57.197	7.433	77.452	44.664	0.92	1.136	5.481
M2-06	0	109.902	0.93	6.048	12.839	2.995	8.952	1.183	49.732	3.287	1.841	3.262
M3-01	0	58.664	1.503	58.154	45.198	2.968	13.982	4.85	43.648	4.649	0.738	11.874
M3-02	0	2.937	2.856	40.881	39.104	0	8.992	3.158	35.496	5.411	0.245	15.086
M3-03	0	23.954	1.87	14.38	18.429	0	7.424	2.251	15.953	1.927	2.351	1.774
M4-01	589.475	79.546	2.124	13.903	16.056	0.734	6.109	4.598	17.143	3.222	1.019	1.468
M4-02	179.262	135.404	1.274	41.599	21.055	7.828	12.432	0	19.111	1.19	1.003	7.696
M5-01	56.64	92.35	3.13	38.92	21.85	21.53	23.04	21.45	103.41	16.95	0.27	0.66
M5-02	88.482	23.69	1.188	59.172	27.691	31.292	37.416	67.71	85.653	4.64	0.509	8.441
M5-03	0	3727.28	6.077	180.264	73.236	0	91.89	4.022	114.517	5.562	0.141	12.336
M5-04	198.824	34.957	1.371	78.339	54.423	15.194	31.645	3.41	59.384	1.779	1.986	18.363
M5-05	38.462	248.612	3.362	138.402	97.922	0	40.08	0	58.097	7.065	0.613	23.923
M5-06	167.731	86.353	0.645	283.728	57.358	91.836	58.617	38.215	137.223	2.843	0.447	15.908

Table 8. Trace element values (part 2) for 23 samples from the Meridian Sand. All values are in ppm.

Sample ID	Rb	Sr	Y	Zr	Nb	Mo	Ba	W	Pb	Th	U
M1-01	19.271	14.008	17.601	760.097	11.302	0	0	0.858	9.452	5.171	-0.057
M1-02	14.828	13.14	6.237	154.499	2.037	0	140.507	1.23	7.275	4.186	-0.049
M1-03	47.86	44.638	27.018	874.45	30.757	0	124.61	1.05	23.068	13.014	-0.155
M1-04	50.25	40.948	25.775	499.262	27.012	0	11.539	0.555	16.308	13.632	-0.172
M1-05	6.957	7.386	4.04	100.575	0	0	0	0.532	6.654	1.475	-0.017
M1-06	12.513	11.317	7.124	280.664	4.483	0	22.246	1.896	6.837	2.396	-0.036
M2-01	13.182	9.425	9.079	353.73	6.531	0	6.173	1.315	8.072	3.103	-0.055
M2-02	40.72	35.099	35.348	210.392	21.135	0	207.46	0.176	19.386	9.766	-0.133
M2-03	6.685	6.867	15.941	357.225	2.772	0	10.719	1.126	0.747	1.974	-0.005
M2-04	15.027	8.009	7.955	341.605	3.683	0	0	1.231	7.057	3.596	-0.051
M2-05	11.85	5.115	11.152	104.72	1.175	0	7.013	0.836	8.668	3.342	-0.04
M2-06	8.909	12.694	15.622	463.458	7.498	0	21.534	1.316	8.802	2.091	-0.018
M3-01	25.826	10.711	8.029	362.604	2.867	0	104.84	1.319	7.642	7.329	-0.099
M3-02	17.773	10.879	10.188	229.467	0	0	28.112	0.896	10.198	4.669	-0.075
M3-03	15.995	4.916	7.449	135.333	0.033	0	15.183	1.073	2.965	3.781	-0.061
M4-01	11.658	12.664	9.413	275.325	2.876	0	20.661	0.644	3.31	2.891	-0.024
M4-02	21.485	16.187	6.214	181.231	2.149	0	35.955	0	10.73	5.077	-0.08
M5-01	83.17	43.24	32.74	207.01	11.86	0	105.45	0	17.32	23.56	-0.3
M5-02	21.804	12.317	21.5	222.913	4.212	0	165.531	0.546	1.161	6.187	-0.095
M5-03	28.122	28.585	33.122	219.842	2.875	0	504.799	1.657	9.3	6.518	-0.085
M5-04	22.753	21.51	21.53	602.056	4.37	0	0	1.236	12.873	5.545	-0.072
M5-05	24.359	30.797	11.054	327.271	4.664	0	0	1.004	15.101	5.827	-0.063
M5-06	16.892	28.669	29.45	66.074	0.209	0	102.048	0	0	1.13	-0.068

APPENDIX IV
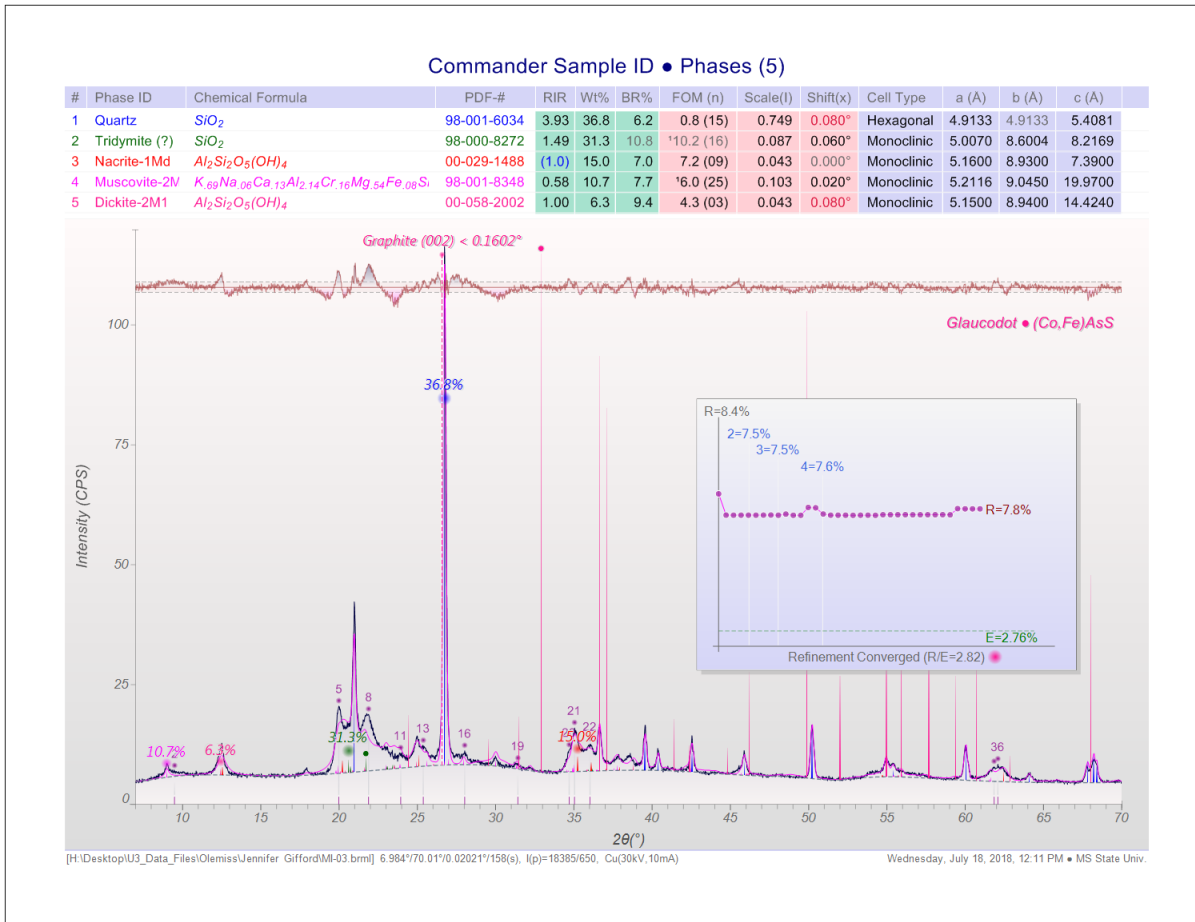
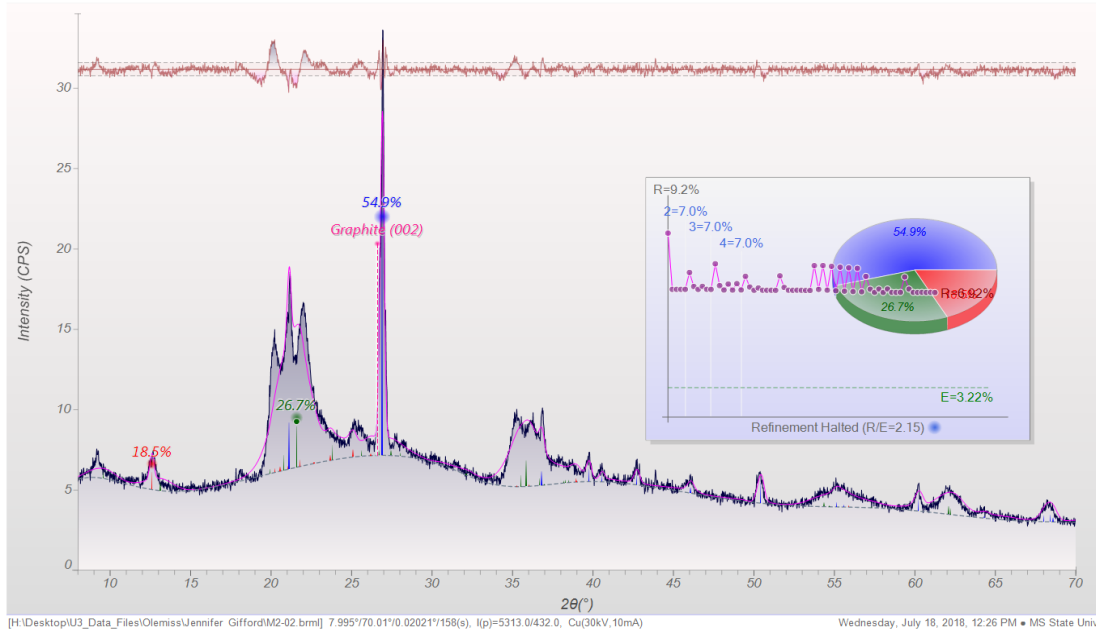Figure 42. XRD data for sample M2-02.

Figure 43. XRD data for sample M1-03.

VITA

Husamaldeen Zubi was born in Albyada City, Libya. He grew up in this city and had lived in it since he was born. In 2007, he attended the department of Geology in Omer El-Mukhtar University, Albyda, Libya. In last year of his undergrad, Husham worked on a small project that focused on carbonate rocks in Aljabal-Elakhdar district. In 2010, Husam achieved his bachelor's degree in Geological science.

In 2012, Husam got an offer from the Geology department at Omer El-Mukhtar University two work as a Teaching Assistant. He has held this position for two years. In 2015, Husam was awarded a full scholarship from the Libyan government, and he traveled to the US to achieve his master degree in Geology. At the current time, he is working as a teaching assistant at the University of Mississippi teaching Mineralogy and Petrology.